

## Green's-matrix calculation of total energies of point defects in silicon

P. J. Kelly

*Philips Research Laboratories, P. O. Box 80.000, 5600 JA Eindhoven, The Netherlands*

R. Car

*IRRMA, PHB-Ecublens, CH-1015 Lausanne, Switzerland  
and Department of Condensed Matter Physics, University of Geneva,  
24 quai E. Ansermet, CH-1211 Geneva 4, Switzerland*

(Received 15 April 1991; revised manuscript received 11 September 1991)

The principal approximation in the Green's-matrix method for calculating the electronic structure and total energy of point defects in crystalline solids is the choice of (finite) basis set. In this paper the results of total-energy calculations with a number of different Gaussian-orbital basis sets are presented for several defects in silicon, including the silicon lattice vacancy and the silicon self-interstitial. Particular attention is paid to the convergence of the total energy with respect to the number of atoms included in the defect cluster on which the Green's matrix is represented. Our best estimate for the formation energy of an unrelaxed neutral silicon lattice vacancy is 4.4 eV. In many cases we are interested in calculating the distortion accompanying incorporation of a point defect or the total-energy difference when a defect is displaced. As illustrative examples, the breathing relaxation around the lattice vacancy and the migration energies of the self-interstitial and of interstitial oxygen are examined. It is shown that the atoms surrounding a neutral silicon lattice vacancy relax inwards toward the site of the missing atom. On including this symmetric relaxation and the Jahn-Teller pairing distortion, the formation energy becomes 3.6 eV. Because of the importance of the long-range response to the Jahn-Teller distortion, it was not possible to calculate the pairing energy entirely *ab initio*. For silicon self-interstitials in the empty channels of the silicon lattice, high-temperature (midgap Fermi-level) formation energies of upwards of 4.4 eV are found. The migration energies are strongly charge-state dependent but in general substantially smaller than the formation energies. The self-interstitial displays negative- $U$  behavior, and its electronic structure supports athermal migration. The migration energy for interstitial oxygen is calculated to be 2.5 eV, which is in good agreement with the experimental value.

### I. INTRODUCTION

The success achieved with the local-density approximation (LDA) in describing the energetics of collections of atoms has led to attempts to apply the Hohenberg-Kohn-Sham formalism<sup>1,2</sup> to increasingly more complex problems.<sup>3</sup> A point defect in an otherwise perfect crystal is an example of such a problem.<sup>4</sup> Various schemes such as finite-cluster,<sup>5</sup> periodic-supercell,<sup>6</sup> or Green's-function<sup>7-9</sup> techniques were devised to deal with the inherent difficulties of the defect problem, i.e., the loss of translational invariance in a crystal. In the development of a Green's-function method suitable for the calculation of defect energies, a number of difficulties were encountered in the original Green's-operator formulations that delayed the application of such schemes to realistic defect models. In these formulations the Green's operator for the perturbed system  $\hat{G}$  is expressed in terms of the unperturbed operator  $\hat{G}^0$  via the Dyson equation

$$\hat{G} = \hat{G}^0 + \hat{G}^0(\hat{V} - \hat{V}^0)\hat{G}, \quad (1)$$

where  $\hat{V} - \hat{V}^0$  is the operator representing the defect perturbation. To obtain solutions of Eq. (1) in practice, some approximations are necessary both for  $\hat{G}^0$  and for  $\hat{G}$ . In the defect problem, for example, the operators are expanded in terms of an incomplete set of localized orbitals. This procedure can easily introduce errors in all the quantities representing a defect-induced change if the perturbed and unperturbed problems are not treated with

the same degree of accuracy.

Another difficulty in the Green's-operator approach is associated with the unbound character of the spectrum of the exact Green's operator. The spectral representation of  $\hat{G}^0$  is used in solving Eq. (1). Therefore, even if one is interested in the operator  $\hat{G}$  only over a finite-energy range, a summation over an infinite spectrum is, at least in principle, implied in Eq. (1). The contribution coming from high-energy states of  $\hat{G}^0$  in Eq. (1) decays only very slowly as the inverse of the energy and may be non-negligible. It is not clear how important this is in practical applications.

These difficulties are relevant in total-energy calculations where one is interested in the small total-energy changes induced by a defect, e.g., formation, migration, and lattice-relaxation energies. All of these quantities involve substantial cancellation between individually large contributions, of the order of several tens of electron volts, to obtain energies that can be as small as a few tenths of an electron volt, as in the case of migration barriers and relaxation energies.

In the Green's-matrix approach proposed by Williams, Feibelman, and Lang<sup>10</sup> both the perfect and the perturbed crystals (including lattice relaxation) are treated with the same accuracy in the presence of different kinds of defects. The fundamental approximation in the matrix method lies in the choice of the localized basis sets for the perfect crystal and for the defect calculation. These basis sets are necessarily approximate but can be chosen in

such a way as to describe the ground states of the respective systems with comparable accuracy. In terms of these basis sets, the Schrödinger equations for the perfect and the perturbed crystals become matrix equations having a finite spectrum. Only at this stage are the matrix equations reformulated in Green's-function language in order to obtain a Dyson equation connecting the Green's matrix for the perturbed problem to the one for the perfect crystal. In contrast to the operators appearing in Eq. (1), the matrices used in the present approach provide only an approximate description of our system, but they have the important advantage that no additional approximations are required to solve the matrix Dyson equation, so that the problems mentioned above in connection with the operator scheme are no longer present.

Since the first calculations of total energies for point defects in semiconductors were reported<sup>11-13</sup> there have been numerous further applications.<sup>14</sup> Few details of these calculations for point defects have been published, making it difficult to assess the accuracy of the different methods and the validity of the approximations made. In this paper some aspects of the implementation of the Green's-matrix scheme in a version appropriate for point defects in semiconductors are considered. The convergence problems associated with the method are identified and studied for a number of specific examples.

The principal approximation involved in the Green's-matrix method is the choice of basis set. We therefore begin by calculating the formation energies of lattice vacancies and interstitials with a number of different basis sets. The problems associated with the convergence of the total energy of charged defects are discussed for the examples of a substitutional phosphorus atom and for a charged self-interstitial atom. An important assumption in the matrix method is that incomplete basis sets that do not result in accurate absolute energies may be sufficiently complete so as to give total-energy differences adequately. To see if this is true, we examine the relaxation of the atoms surrounding a lattice vacancy and the migration energy of a self-interstitial with the same basis sets that were used to study the vacancy and interstitial formation energies. These examples illustrate the strengths as well as the weaknesses of the Green's-matrix method. However, none of the energies calculated are well known experimentally. In order to make a comparison with experiment, the migration energy of an interstitial oxygen atom in silicon is calculated.

The paper is organized as follows. In Sec. II, the Green's-matrix scheme for defect calculations is summarized in order to establish the notation used. In Sec. III the results of calculations illustrating the convergence properties of the defect total energy are given. Examples are treated where lattice relaxation is important. A discussion of these results and a comparison with other calculations follows in Sec. IV. In Sec. V a brief summary is given together with our conclusions.

## II. GREEN'S-MATRIX SCHEME FOR DEFECTS IN SOLIDS

Calculation of the total energy within the density-functional formalism<sup>1</sup> requires iterative solution of the

following set of equations:<sup>2</sup>

$$\{-\nabla^2 + V[n_e](\mathbf{r})\}\psi_i(\mathbf{r}) = \varepsilon_i \psi_i(\mathbf{r}), \quad (2)$$

$$n_e(\mathbf{r}) = \sum_i f_i |\psi_i(\mathbf{r})|^2, \quad (3)$$

and

$$V[n_e](\mathbf{r}) = V_{\text{ext}}(\mathbf{r}) + 2 \int \frac{n_e(\mathbf{r}')}{|\mathbf{r}-\mathbf{r}'|} d^3r' + \mu_{\text{xc}}(n_e(\mathbf{r})). \quad (4)$$

Here  $f_i$  are occupation numbers, and  $\mu_{\text{xc}}$ , the exchange-correlation potential, is given within the local-density approximation using the interpolation formula of Ref. 15. We use Rydberg atomic units throughout. In the pseudopotential approach,<sup>16,17</sup> the external potential  $V_{\text{ext}}$  is replaced by an effective potential  $V_{\text{ps}}$ , which represents the interaction of the valence electrons with the nucleus and the (frozen) core electrons. For a collection of atoms on sites  $\mathbf{R}$ ,  $V_{\text{ps}}$  is given by a sum of atomic pseudopotentials:

$$V_{\text{ps}} = \sum_{\mathbf{R}} v_{\text{ps}}(\mathbf{r}-\mathbf{R}). \quad (5)$$

We shall write the wave functions of (2) as a linear combination of Gaussian orbitals,

$$\psi_i(\mathbf{r}) = \sum_{\alpha} c_{i\alpha} \phi_{\alpha}(\mathbf{r}), \quad (6)$$

with the shorthand notation  $\alpha \equiv \{nlm; \mathbf{R}\}$  such that

$$\begin{aligned} \phi_{\alpha}(\mathbf{r}) &= \phi_{nlm}(\mathbf{r}-\mathbf{R}) \\ &= |\mathbf{r}-\mathbf{R}|^l e^{-\gamma_{nl}(\mathbf{r}-\mathbf{R})^2} Y_{lm}(\hat{\mathbf{r}}-\hat{\mathbf{R}}), \end{aligned} \quad (7)$$

where  $Y_{lm}(\hat{\mathbf{r}})$  are spherical harmonics. In principle, any choice of localized orbitals is good, our choice of Gaussian orbitals being determined by their well-documented computational convenience: reciprocal space operations can be carried out simply and efficiently because of the rapid convergence of the Fourier transform of Gaussian orbitals, and multicenter integrals can be evaluated analytically. Gaussian orbitals have been used in all-electron calculations<sup>18,19</sup> and more recently in combination with pseudopotentials.<sup>7,8,20-22</sup> These references only cover applications to extended systems, and the list is representative rather than exhaustive.

In terms of the expansion (6), the differential equations (2) transform into a set of algebraic equations for the coefficients  $c_{i\alpha}$ :

$$\sum_{\beta} (H_{\alpha\beta} - \varepsilon_i S_{\alpha\beta}) c_{i\beta} = 0, \quad (8)$$

with

$$H_{\alpha\beta} \equiv \int d^3r \phi_{\alpha}^*(\mathbf{r}) [-\nabla^2 + V(\mathbf{r})] \phi_{\beta}(\mathbf{r}) = t_{\alpha\beta} + V_{\alpha\beta} \quad (9)$$

and

$$S_{\alpha\beta} \equiv \int d^3r \phi_{\alpha}^*(\mathbf{r}) \phi_{\beta}(\mathbf{r}). \quad (10)$$

The expansion coefficients diagonalize both the Hamiltonian matrix  $H_{\alpha\beta}$  and the overlap matrix  $S_{\alpha\beta}$ :

$$\sum_{\alpha,\beta} c_{i\alpha}^* H_{\alpha\beta} c_{j\beta} = \varepsilon_i \delta_{ij}, \quad \sum_{\alpha,\beta} c_{i\alpha}^* S_{\alpha\beta} c_{j\beta} = \delta_{ij}, \quad (11)$$

where  $\delta_{ij}$  is the Kronecker delta. The expansion (6) is necessarily approximate due to the incompleteness of the basis set  $\{\phi_\alpha(\mathbf{r})\}$ . The only requirement on the basis set is that it should be sufficiently complete to describe the ground state of the system satisfactorily. In other words, only the occupied states need be described correctly in (6). The basis sets used for the perturbed and the unperturbed crystals may be different. This is particularly useful in defect calculations where at the defect site we are free to use the orbitals most appropriate to an impurity atom. When atoms are displaced, it is sufficient to displace the corresponding localized orbitals with the atoms.

Equation (8) can be cast in Green's-function language as follows:<sup>10</sup>

$$\sum_{\beta} (zS_{\alpha\beta} - H_{\alpha\beta}) G_{\beta\gamma}(z) = \delta_{\alpha\gamma}, \quad (12)$$

where the Green's matrix for complex energy  $z$  is given by

$$G_{\alpha\beta}(z) = \sum_i \frac{c_{i\alpha} c_{i\beta}^*}{z - \epsilon_i} \quad (13)$$

in terms of the eigenvalues  $\epsilon_i$  and the eigenvectors  $c_{i\alpha}$  of (8). Equation (12) is completely equivalent to (8). From the Green's function one can construct the density matrix:

$$\rho_{\alpha\beta} = \frac{1}{2\pi i} \int_{c(\epsilon_F)} dz G_{\alpha\beta}(z) = -\frac{1}{\pi} \int_{-\infty}^{\epsilon_F} d\epsilon \operatorname{Im} G_{\alpha\beta}(\epsilon). \quad (14)$$

The contour  $c(\epsilon_F)$  in (14) encloses all the occupied one-electron states and therefore crosses the real axis at the Fermi energy  $\epsilon_F$ . From the density matrix one can obtain the electron density

$$n_e(\mathbf{r}) = \sum_{\alpha, \beta} \phi_\alpha(\mathbf{r}) \rho_{\alpha\beta} \phi_\beta^*(\mathbf{r}) \quad (15)$$

and all the quantities that are needed to perform a self-consistent iteration and compute the total energy.

We describe an unperturbed system characterized by a potential  $V^0(\mathbf{r})$  with a basis set  $\{\phi_\alpha^0(\mathbf{r})\}$  and a perturbed system characterized by a potential  $V(\mathbf{r}) = V^0(\mathbf{r}) + \Delta V(\mathbf{r})$  with a basis set  $\{\phi_\alpha(\mathbf{r})\}$ . The matrix elements of the perturbing potential  $\Delta V(\mathbf{r})$  are given by

$$\Delta V_{\alpha\beta} \equiv \int d^3r [\phi_\alpha^*(\mathbf{r}) V(\mathbf{r}) \phi_\beta(\mathbf{r}) - \phi_\alpha^0(\mathbf{r}) V^0(\mathbf{r}) \phi_\beta^0(\mathbf{r})]. \quad (16)$$

The Green's matrix  $G(z)$  characterizing the perturbed

system is related to the Green's matrix  $G^0(z)$  characterizing the unperturbed system via the following Dyson equation:<sup>10</sup>

$$G(z) = G^0(z) + G^0(z)(\Delta H - z\Delta S)G(z), \quad (17)$$

where the subscripts have been suppressed for simplicity. In (17),  $\Delta H = H - H^0 = \Delta t + \Delta V$  and  $\Delta S = S - S^0$  indicate matrix differences. Note that the perturbation in (17) does not depend only on the physical perturbation  $\Delta V = V - V^0$  as it does in the operator formulation (1), but it also includes the dependence on the basis-set change explicitly. This additional perturbation can be of longer range than the real physical perturbation.

Due to the loss of translational invariance in the defect problem, the direct solution of the infinite set of algebraic equations (8) or (12) is in general not possible. However, the Dyson-equation formulation (17) allows one to compute the quantities of physical interest by solving finite sets of algebraic equations, provided the perturbation induced by a defect is localized, i.e., it has the form

$$\begin{aligned} \Delta H - z\Delta S &= \begin{pmatrix} (\Delta H - z\Delta S)_{AA} & (\Delta H - z\Delta S)_{AB} \\ (\Delta H - z\Delta S)_{BA} & (\Delta H - z\Delta S)_{BB} \end{pmatrix} \\ &= \begin{pmatrix} (\Delta H - z\Delta S)_{AA} & 0 \\ 0 & 0 \end{pmatrix}, \end{aligned} \quad (18)$$

where the subspace  $A$  is finite. The solution of (17) is given by

$$G(z) = [1 - G^0(z)(\Delta H - z\Delta S)]^{-1} G^0(z). \quad (19)$$

The matrix difference  $\Delta G(z) = G(z) - G^0(z)$  is in general not restricted to the subspace  $A$ . On the contrary, the changes in the individual wave functions or in the density matrix are usually considerably more extended than the small subspace  $A$  that is used in practical applications. However, if (18) is satisfied, the change in the density of states as well as the change in the sum of the occupied one-electron eigenvalues  $\Delta(\sum_i f_i \epsilon_i)$  can be obtained *exactly* from algebraic manipulations involving only the finite subspace  $A$ .<sup>23,24</sup> This follows from the identity

$$\begin{aligned} \operatorname{Tr}[G(z)S] &\equiv \operatorname{Tr} \left[ (zS - H)^{-1} \frac{d}{dz} (zS - H) \right] \\ &\equiv \frac{d}{dz} \operatorname{Tr} \ln(zS - H). \end{aligned} \quad (20)$$

Using (20), one obtains<sup>23,24</sup> the following expressions for the change in the density of states  $\Delta N(z)$ :

$$\begin{aligned} \Delta N(z) &\equiv \frac{1}{2\pi i} \{ \operatorname{Tr}[G(z)S] - \operatorname{Tr}[G^0(z)S^0] \} = -\frac{1}{2\pi i} \operatorname{Tr} \left[ \left[ \frac{d}{dz} G^0(z)(\Delta H - z\Delta S) \right] [1 - G^0(z)(\Delta H - z\Delta S)]^{-1} \right] \\ &= -\frac{1}{2\pi i} \operatorname{Tr} \left[ \left[ \frac{d}{dz} G_{AA}^0(z)(\Delta H - z\Delta S)_{AA} \right] [1 - G_{AA}^0(z)(\Delta H - z\Delta S)_{AA}]^{-1} \right] \\ &= \frac{1}{2\pi i} \frac{d}{dz} \ln \det [1 - G_{AA}^0(z)(\Delta H - z\Delta S)_{AA}]. \end{aligned} \quad (21)$$

In any of its equivalent forms, (21) is restricted to the subspace  $A$  as a consequence of (18). The total change in the number of states  $\Delta N$  and the change in the sum of the occupied eigenvalues are given in terms of  $\Delta N(z)$  by

$$\Delta N = \int_{c(\varepsilon_F)} dz \Delta N(z) \quad (22)$$

and by

$$\Delta \left( \sum_i f_i \varepsilon_i \right) = \int_{c(\varepsilon_F)} dz z \Delta N(z), \quad (23)$$

respectively. Both  $\Delta N(z)$  and  $\Delta(\sum_i f_i \varepsilon_i)$  are therefore restricted to the subspace  $A$ .

The change in the electron density  $\Delta n_e(\mathbf{r})$  is related via (15) to the change in the density matrix  $\Delta \rho$ , which is a quantity not necessarily restricted to the subspace  $A$ . However, since in a self-consistent calculation the change in the total electron density  $\Delta n_e(\mathbf{r})$  cannot have longer range than the total potential it gives rise to, it is sufficient to compute  $\Delta \rho$  in the subspace  $A$ , i.e.,  $\Delta \rho_{AA}$  to obtain  $\Delta n_e(\mathbf{r})$  in a way that is consistent with the assumption (18).<sup>7</sup>

So far, all the elements needed to perform a full self-consistent calculation have been given using only expressions that involve finite matrices. At a given iteration, (22) is used to define the contour  $c(\varepsilon_F)$ , then  $\Delta \rho_{AA}$  is computed using (19) and (14). From (15) we then obtain  $\Delta n_e(\mathbf{r})$ , which is represented numerically on a cubic real-space mesh. Poisson's equation is solved using fast Fourier transforms (FFT's) to find the Hartree component of the new potential  $\Delta V(\mathbf{r})$ , which is represented on the same cubic mesh.<sup>7</sup> The exchange-correlation potential is evaluated numerically on the mesh. Matrix elements of the perturbation  $\Delta t_{\alpha\beta}$ ,  $\Delta S_{\alpha\beta}$ , and, where practicable, of  $\Delta V_{\alpha\beta}$ , are evaluated analytically; otherwise, they are calculated numerically by numerical summation of the integral in (16). Full use is made of the point-group symmetry to calculate the unperturbed Green's matrix, to calculate matrix elements of the perturbing potential, and to solve the Dyson equation (19). Contour integration in the complex plane is advantageous over energy integration along the real axis, since the Green's function varies rapidly on the real axis, whereas it is well behaved and smooth for complex energy values.<sup>25,10</sup> All the necessary sums over the occupied states are carried out by numerical integration around a contour in the complex energy plane. When self-consistency is achieved, the change in the density of states<sup>26</sup> can be obtained from (21), and the single-particle contribution to the total-energy difference from (23). Further technical aspects of the evaluation of the total energy with the local-density approximation using first-principles Green's-function schemes, which have been discussed in the literature,<sup>27-29</sup> will not be discussed further here.

According to (18), all long-range effects are neglected as if the self-consistent potentials for all defects were completely screened. This is, however, incorrect, since in a semiconductor the potential of a charged defect has a long-range Coulombic tail and even the potential of a neutral defect generally contains some long-range multipole contributions falling off with distance as some in-

verse power of  $r$ . Neither is  $\Delta n_e(\mathbf{r})$ , in principle, completely localized, since it contains some small long-range oscillatory contributions.<sup>30</sup> It is certainly not possible to follow these long-range effects all the way out numerically. However, many physical quantities depend only weakly on these long-range effects, and converge rapidly as  $r \rightarrow \infty$ . It is therefore a perfectly permissible procedure to truncate the potential  $\Delta V(\mathbf{r})$ , i.e., to restrict the matrix  $\Delta V$  to a finite subspace  $A$  and to compute all the quantities of physical interest using this truncated potential, in which case neither numerical nor analytical problems arise. By varying the dimension of the subspace  $A$ , it is then possible to monitor the convergence of the various physical quantities we want to compute. What makes this procedure practicable in the defect problem is the fact that usually the relevant dimension of  $A$  is small and numerically manageable.

We want to make a comment on a special feature of the Green's-matrix scheme that illustrates the great flexibility of the method. In writing (17), we implicitly assumed that the perturbed and unperturbed basis sets have the same dimensions. At first this may appear to be a serious limitation of the method, since in many problems, e.g., an interstitial impurity or a substitutional transition atom impurity in an  $sp$  host, the perturbed basis set is larger than the unperturbed one. However, the difficulty is only apparent, since it is very easy by means of the so-called *adspace*<sup>10</sup> concept to construct a fictitious  $G^0$  having the appropriate dimension for the matrix equation (17).

For instance, a suitable  $G^0$  for an interstitial impurity is given by the matrix

$$G^0(z) = \begin{pmatrix} G_A^0(z) & 0 \\ 0 & G_C^0(z) \end{pmatrix}. \quad (24)$$

$G_C^0$  is the unperturbed crystal Green's matrix and  $G_A^0$  is a Green's matrix for the impurity *adatom*. Notice that it is *not* required that  $G_A^0$  should describe a real atom.  $G_A^0$  should only have the right dimension and have a form that makes it easy to construct an appropriate perturbation  $\Delta H - z\Delta S$  to bring the initial fictitious system into the final physical one. In our implementation we find it convenient to use the following definitions for the adatom Hamiltonian and Green's matrices:

$$(H_A^0)_{\alpha\beta} \equiv \varepsilon_A \delta_{\alpha\beta}, \quad (S_A^0)_{\alpha\beta} \equiv \delta_{\alpha\beta}, \quad (25)$$

$$(G_A^0)_{\alpha\beta}(z) \equiv \frac{1}{z - \varepsilon_A} \delta_{\alpha\beta}, \quad (26)$$

where we choose  $\varepsilon_A$  to lie in the conduction bands of the unperturbed crystal in order to avoid adatom contributions to the unperturbed density matrix (and electron density).

Another problem can arise when the perturbed system consists of fewer atoms than the unperturbed one, as for example in the case of a vacancy. Here the unperturbed system contains orbitals on the vacant site, where they are not needed in the perturbed system. In this case, it is possible to reduce the dimension of the unperturbed Green's matrix by means of the so-called *ideal*<sup>10</sup> concept.

This consists of decoupling the orbitals centered on the vacancy site from the rest of the problem, so that (17) is solved in a space having reduced dimensions. The unperturbed Green's matrix in such a problem is the so-called ideal Green's matrix.

We refer to the original paper by Williams, Feibelman, and Lang<sup>10</sup> for a more rigorous definition of the ideal Green's matrix. This mathematical construction is only really needed when the dimension of the subspace that we want to decouple is itself infinite, as in the case of a surface. In the vacancy problem where the dimension of this subspace is finite, we can achieve the same result numerically, with a much simpler computational procedure. Indeed, the ideal construction is equivalent to introducing a perturbation of the form

$$U_{\alpha\beta} \equiv u \delta_{\alpha\beta}, \quad u \rightarrow \infty, \quad (27)$$

where  $\alpha$  or  $\beta$  is one of the orbitals that we want to eliminate. Rather than performing the limit implied in (27) analytically, we can obtain the same result numerically by simply adding a potential of the form (27) with a finite but very large  $u$  in our calculation. The ideal Green's-matrix scheme was implemented and yielded the same result for the vacancy formation energy within the numerical precision of the calculation.

In the calculations to be discussed in this paper, nonlocal norm-conserving pseudopotentials<sup>16</sup> were constructed by fitting the results of an all-electron atomic calculation following the scheme given in Ref. 31. According to this scheme,  $v_{ps}$  is written in terms of a long- and a short-range component:

$$v_{ps}(\mathbf{r}) = v_{ps}^{\text{LR}}(\mathbf{r}) + v_{ps}^{\text{SR}}(\mathbf{r}), \quad (28)$$

where

$$\begin{aligned} v_{ps}^{\text{LR}}(\mathbf{r}) &= -\frac{2Z_v}{r} \operatorname{erf}\left(\frac{r}{r_n}\right) \\ &= \int \left[ \frac{-2Z_v}{\pi^{3/2} r_n^3} \right] \frac{e^{(-r'^2/r_n^2)}}{|\mathbf{r}-\mathbf{r}'|} d^3r', \end{aligned} \quad (29)$$

and

$$v_{ps}^{\text{SR}}(\mathbf{r}) = \sum_l (a_l + b_l r^2) e^{(-r^2/r_{cl}^2)} \hat{P}_l = \sum_l v_l(r) \hat{P}_l. \quad (30)$$

Here  $Z_v$  is the atomic valence charge, and  $\hat{P}_l$  are projection operators over the angular momentum states  $l$ .  $r_n$  and  $r_{cl}$  are core radii depending on the particular atom being considered, and  $a_l$  and  $b_l$  are fitting parameters (two for each  $l$  value). Explicit values of these parameters and of the core radii are given in Table I for Si, P, and O.

### III. CALCULATIONS

There are two basic convergence issues we can identify: one is convergence with respect to the number of atomic sites that must be included in the self-consistent calculation for a given set of basis functions. When the energy is converged in this respect it can be compared to the energy calculated using a better basis set. The criterion for

TABLE I. Values of the pseudopotential parameters defined in (30) for silicon, phosphorus, and oxygen in Rydberg atomic units.

	$l$	$a_l$	$b_l$	$r_{cl}$
Silicon $r_n=1.09$	0	20.3046	-10.4769	0.81
	1	5.6365	-2.3370	0.92
	2	-9.8525	2.4567	1.00
Phosphorus $r_n=0.90$	0	28.4798	-15.6429	0.71
	1	10.0363	-4.3686	0.77
	2	-14.6143	5.1056	0.82
Oxygen $r_n=0.50$	0	47.4309	-112.6213	0.40
	1	-41.6811	25.8710	0.33

the quality of a particular basis set is its ability to minimize the total energy. These two aspects are to a large extent independent, since the spatial extent of the physical perturbation ought not to depend strongly on the basis set used in the calculation. We will discuss the unrelaxed silicon lattice vacancy and substitutional phosphorus in silicon as examples of where this is true. In the Green's-matrix scheme there is the additional complication that the perturbation depends explicitly on the basis-set change, via the terms  $\Delta t$  and  $\Delta S$  in (17). Depending on the decay lengths of the orbitals used, this can introduce an effective perturbation that is longer range than the physical perturbation. As examples of this case we will discuss the tetrahedral self-interstitial in silicon and the breathing relaxation about the silicon lattice vacancy.

We consider the following specific defects, namely the substitutional  $P^+$  impurity, the neutral and doubly positively charged lattice vacancies  $V^0$  and  $V^{2+}$ , the self-interstitial  $I$  at tetrahedral and hexagonal symmetry sites, and interstitial oxygen, all in silicon. These defects represent different prototypical cases. The  $P^+$  impurity is an example of a weak, long-range perturbation. Both  $V^0$  and  $I^0$  are strong localized perturbations, one (the self-interstitial) requiring the adspace construction, the other (the vacancy) may be calculated with or without the reduced space construction. The charged self-interstitial  $I^{2+}$  is an example of a strong, long-range perturbation. Interstitial oxygen is an example of a strong short-range perturbation accompanied by a large lattice distortion. By calculating the lattice relaxation of the vacancy and the migration energies of the self-interstitial and interstitial oxygen with different basis sets, we will see how well energy differences are described when an incomplete basis set is used for which the total energy is far from the converged value.

For vacancies and self-interstitials, the usual quantity of physical interest is the formation energy, which is defined for the vacancy as

$$E_F(V) \equiv \Delta\Omega(V) + E_{\text{Si}}^*, \quad (31)$$

and for the self-interstitial as

$$E_F(I) \equiv \Delta\Omega(I) - E_{\text{Si}}^*, \quad (32)$$

where  $E_{\text{Si}}^*$  is the total energy of a silicon pseudoatom in

the perfect crystal.  $\Delta\Omega$  is given in terms of the sum of the electronic and ionic contributions to the energy of the defect  $\Delta E$ ,

$$\Delta\Omega \equiv \Delta E - \mu\Delta N, \quad (33)$$

where  $\mu$  is the chemical potential (the Fermi level) and  $\Delta N$  [Eq. (22)] indicates the electrons added to or subtracted from the defect in order to get its appropriate charge state. In other words, one has to allow for the possibility for the defect to exchange electrons with a reservoir of noninteracting electrons at the Fermi energy in order to obtain a charge state different from the neutral one.

The difference in formation energies at two different sites that correspond to energy maxima and minima along a possible diffusion path represents a migration energy  $E_M$ . For an impurity atom the heat of solution is defined as

$$E_F(P) \equiv \Delta\Omega(P) - (E_P - E_{Si}). \quad (34)$$

Here  $E_P$  and  $E_{Si}$  are total energies of pseudoatoms in free space.

#### A. Pseudopotentials and basis sets

In the calculations reported in this paper, norm-conserving pseudopotentials of the form (28)–(30) for silicon, phosphorus, and oxygen have been used. Appropriate values for the pseudopotential parameters and for the core radii of these elements are given in Table I.

In choosing a basis set we must try to satisfy two (possibly) conflicting requirements. The first requirement is that the basis functions should be as *short* range as possible in order that the change-of-basis perturbations  $\Delta S$  and  $\Delta t$  should be short range. The second requirement is that the basis set should contain functions that are sufficiently *long* range so that it can describe the atom in all configurations that are likely to be encountered, including atomiclike configurations, where it may be necessary to be able to describe the long-range “tail” of the atom. An example of the latter is the undercoordinated atoms of the simple vacancy. In addition, there should be

as few basis set orbitals as possible to enable large clusters to be treated. In practice it is difficult to satisfy all of these conditions simultaneously. The main problem arises when we want to relax the atoms around a defect. This introduces a physical perturbation that is fairly well localized around the atoms that are disturbed. If the basis functions being used have long range, the change-of-basis perturbation may then dominate and require a calculation with a very large cluster of atoms.

All our calculations were carried out using Gaussian orbitals. We tabulate in Table II five representative basis sets for silicon as characterized by the exponents  $\gamma_{nl}$  (7). The values of the ground-state properties of the perfect silicon crystal calculated with these basis sets together with the results of an essentially converged plane-wave calculation are also listed.<sup>31</sup>

The first and crudest basis set comprises two *s* and two *p* Gaussian orbitals. The exponents 0.2 and 0.5 (in units of  $a_0^{-2}$ , where the Bohr radius  $a_0 = 0.529 \text{ \AA}$ ) are those exponents used in our first calculations of defect total energies.<sup>12</sup> The second basis set demonstrates how the total energy can be lowered by reducing the range of the short-range *s* orbital. The short-range *p* orbital has only a small effect on the energy, and it is economical to omit it entirely. We have found that for Si it is advantageous to include more *s* orbitals than *p* orbitals for a given bound on the maximum range of the basis functions. This may be simply understood in terms of the nodal form of the Gaussian orbitals and the form of the pseudo-wave functions. The third basis set has the same *s*- and *p*-orbital exponents as set II, and in addition contains a *d* orbital. The exponent of this orbital has been chosen so as to minimize the total energy of the perfect crystal. The fourth basis set was constructed with three *s* and two *p* orbitals whose exponents were determined by (approximately) minimizing the total valence energy of the free silicon atom subject to the longest-range orbital having an exponent  $\gamma \geq 0.14$ . Again, it was found that there was very little to be gained by including an additional *p* orbital with exponent greater than 0.14. The fifth basis set has the same *s*- and *p*-orbital exponents as basis set IV and in addition contains a *d* orbital whose ex-

TABLE II. Comparison of calculated ground-state properties for different basis sets as described in the text. The basis sets are characterized by the set of exponents  $\{\gamma_{nl}\}$ . The plane-wave calculation was carried out with a plane-wave kinetic-energy cutoff of 20 Ry. The lattice constant  $A$  and the bulk modulus  $B$  were calculated by fitting the energies calculated at five lattice constants with a parabola. Because of the very small energy differences involved, the determination of  $B$ , in particular, was not very accurate.

Basis set	$\gamma_{nl}$						$A$ ( $a_0$ )	$B$ (Mbar)	$E$ (Ry)
	$l=0$		$l=1$		$l=2$				
I	0.20	0.50	0.20	0.50			10.18	1.07	−7.811
II	0.20	0.80	0.20				10.28	1.04	−7.840
III	0.20	0.80	0.20		0.20		10.39	0.9	−7.867
IV	0.14	0.40	1.00	0.14	0.40		10.48	0.69	−7.899
V	0.14	0.40	1.00	0.14	0.40	0.40	10.25	0.95	−7.930
400 PW							10.20	0.93	−7.949
Expt.							10.263	0.99	

ponent was chosen so as to minimize the total energy of the perfect crystal. It is interesting to note that the resulting exponent  $\gamma_d$  is different from that found for basis set III.

Although even the worst basis set (I) yields 98.3% of the total crystal valence energy, the remaining 1.7% amounts to 0.138 Ry (=1.9 eV). The possibility of obtaining more precise results for energy *differences* with such incomplete basis sets is one of the principle proposed advantages of the matrix method.<sup>10</sup> In this scheme both the unperturbed and the perturbed systems are treated in such a way as to maximize the cancellation of errors when calculating the difference in energy. Care must be taken in choosing a basis set that is suited to the particular problem in hand. This may not always be immediately obvious. For example, on removing an atom to form a vacancy it might be argued that the orbitals of that atom should also be removed, as discussed in Sec. II. We will see later on that the orbitals in basis sets I and II, while capable of describing the perfect crystal reasonably well, do not describe the (second-nearest-neighbor) interaction between the dangling bonds of the four atoms neighboring the vacant site very well. In this case, including orbitals on the vacant site allows this interaction to be described, but introduces an uncontrolled error in the absolute value of the defect energy by abandoning the spirit of the matrix scheme, namely, that there should only be orbitals centered on atoms. Alternatively, we can use basis sets IV or V, which contain longer-range orbitals. It will be seen that the formation energy is then considerably less sensitive to additional orbitals on the vacancy site, confirming that these basis sets describe the dangling-bond interaction correctly. Basis set III, obtained by augmenting basis set II with a long range  $d$  orbital, also gives a good description of the vacancy. In order to calculate the formation energy of the tetrahedral self-interstitial reasonably well, we shall find it necessary to include orbitals with  $d$  angular momentum character.

One might ask, what Gaussian orbital basis set  $\{\gamma_{nl}\}$  is capable of yielding as good a description of the ground-state properties of bulk silicon as given by 400 plane waves? While we cannot give a definitive answer to this question, we have found that adding one more  $p$  or  $d$  orbital whose exponent lies in the range 0.14–1.00 only reduces the total energy per atom by a few mRy. Use of exponents with longer range ( $\gamma < 0.14$ ) led to a small reduction of the crystal energy, but in calculations for defects, this advantage was offset by problems arising from the resulting long-range change-of-basis perturbation. For example, calculations for the silicon tetrahedral self-interstitial with a basis set including an orbital exponent  $\gamma_s = 0.1$  were only converged with a cluster of 67 sites. To demonstrate this convergence, it was necessary to perform a calculation for a cluster including 83 sites. There was no significant difference in the formation energies calculated with this basis set and the basis set IV described above. We conclude that basis set V can only be improved significantly by using a  $\{4 \times s, 3 \times p, 2 \times d\}$  basis, whose longest-range exponents are less than 0.14. We note that basis set V gives a total crystal energy as low as that obtained with about 200 plane waves per unit

cell. In a plane-wave calculation, an additional 200 plane waves are required to reduce the total energy by the remaining 19 mRy.

There is no single commonly accepted way of choosing the Gaussian-orbital exponents.<sup>7,8,20–22,32,33</sup> All of these authors, with the exception of Feibelman, use individual uncontracted atom-centered Gaussian orbitals as basis states. Rather than choosing the exponents so as to fit the eigenvalue spectrum<sup>20,33</sup> or the atomic pseudo-wave function,<sup>32,33</sup> we have chosen them so as to minimize the total energy,<sup>21,22</sup> since this is the quantity we are primarily interested in. The lack of a systematic way of improving the Gaussian-orbital basis is probably its most important shortcoming.

The use of contractions of Gaussians as well as non-atom-centered (floating) orbitals has recently been advocated by Feibelman,<sup>33</sup> although earlier work found single atomic orbitals inadequate for describing the valence wave functions in solids<sup>19</sup> and that atom-centered Gaussians yielded a simpler and more accurate description of the eigenvalue spectrum than floating orbitals.<sup>20</sup>

### B. The unrelaxed neutral lattice vacancy

In this section we begin by examining the convergence with respect to cluster size of the formation energy of the ideal neutral lattice vacancy, where the four nearest-neighbor atoms occupy perfect lattice sites. Their relaxation will be discussed in Sec. III E. To examine the convergence with respect to cluster size, we proceed as follows. A cluster is defined by all the atoms within a shell of some radius about the defect center. For the lattice vacancy there are shells containing 4, 12, 12, 6, 12, 24, . . . atoms at radii of, respectively, 4.443, 7.255, 8.507, 10.260, 11.181, 12.566, . . .  $a_0$  from the tetrahedral site and they define clusters of 5, 17, 29, 35, 47, 71, . . . atoms (where the central vacant lattice site is included in the count). The Green's matrices, perturbing potential, and change in charge density are all represented in terms of the orbitals centered on these sites. The representation of these quantities on a regular mesh in real space then necessarily requires that the mesh be as extended as the longest-range orbitals on the outermost atoms of the cluster, as discussed in Sec. II. The formation energy for the vacancy (31), calculated using basis set II, is plotted as a function of the cluster radius in Fig. 1. The total energy is seen to be essentially converged for a cluster of 17 atoms: inclusion of an additional shell of atoms leads to a change in the energy of 0.5 mRy. The energy changes by less than 0.1 mRy for clusters of 35, 47, and 71 atoms.

The calculations shown in Fig. 1 were carried out retaining on the vacancy site the orbitals of the silicon atom that was removed to form the vacancy. As discussed in Sec. II, it is possible to perform the calculation without these orbitals. Doing this reduces the variational freedom, and the resulting formation energy is 0.039 Ry larger. It is not *a priori* clear which of these formation energies is the more reliable, since the energy under consideration is an energy *difference* to which variational arguments cannot be applied. The source of the problem lies in the incompleteness of the basis set II. In Fig. 2,

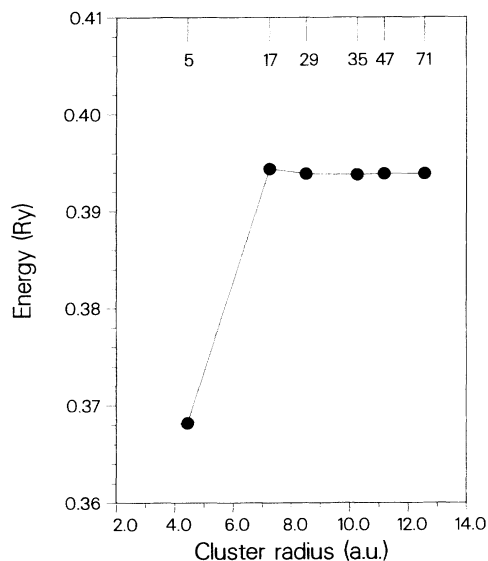


FIG. 1. Formation energy of the neutral lattice vacancy as a function of the radius of the cluster on which the perturbation is represented in the Green's-matrix formalism. The calculations were performed with basis II and orbitals were included on the vacant lattice site. The number of atoms included in each calculation is indicated on the upper horizontal axis. Lattice relaxation was not included, and the defect has tetrahedral symmetry.

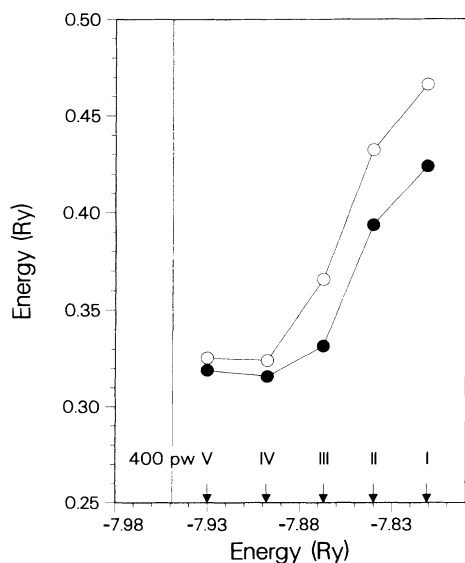


FIG. 2. Formation energy of the neutral lattice vacancy for the different basis sets detailed in Table II. For each basis set, the total energy was converged with respect to the cluster size to better than 1 mRy. The x coordinate is the total energy per Si atom for the perfect crystal. The values calculated with the five different basis sets are indicated by arrows. For comparison the total energy obtained for the perfect crystal with a plane-wave basis is included. Calculations where the basis functions on the vacant site were removed (retained) are denoted by open (closed) circles.

$E_F(V^0)$  as calculated with all five basis sets detailed in Table I is plotted as a function of the crystal energy corresponding to the same basis set. Each calculation is converged to better than 0.0005 Ry with respect to cluster size. For all basis sets, a 29-atom cluster is sufficient to achieve this degree of convergence. The calculations were carried out with and without orbitals on the vacancy site.

The most noteworthy features of Fig. 2 are that (i)  $E_F(V^0)$  decreases as the basis set is improved and appears to level off to a value of about 0.32 Ry, and (ii) the effect of removing the orbitals on the vacancy site diminishes to a value of 7 mRy for basis set V. This is one measure of the degree of convergence of  $E_F(V^0)$ . A more conservative measure of the absolute convergence error of the vacancy formation energy is 19 mRy, or the amount by which the total energy for a lattice atom may be reduced for a fully converged basis set.

Our best estimate for the formation energy of a neutral unrelaxed vacancy is between 0.319 and 0.326 Ry. This energy is independent of the position of the Fermi energy  $\mu$ . For the unrelaxed doubly ionized vacancy  $V^{2+}$ , our best estimate of the formation energy lies between 0.271 and 0.280 Ry, where the Fermi level is taken to be pinned at the top of the valence band ( $\mu=0$ ).

### C. Charged defects

The results of  $\Delta E(P^+)$  for the ionized substitutional phosphorus impurity obtained with basis set IV for various cluster sizes are given in Fig. 3. In order to eliminate the "change-of-basis perturbation," the same basis is used here on the P and Si atoms. The long-range nature of the perturbation is apparent by comparison with Fig. 1. The energy increases monotonically with each shell of atoms added, although the absolute increase in the total energy

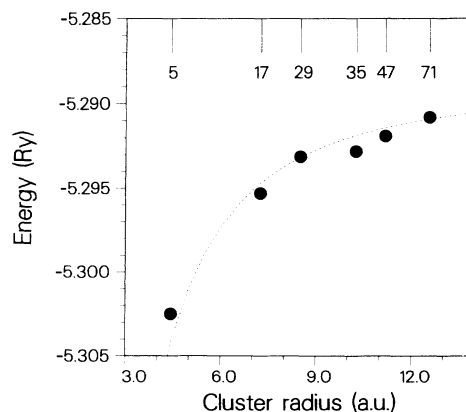


FIG. 3. Total-energy difference for an ionized substitutional phosphorus impurity atom in silicon as a function of the radius of the cluster on which the perturbation is represented in the Green's-matrix formalism. The calculations were performed with basis set IV. The number of atoms included in each calculation is indicated on the upper horizontal axis. Lattice relaxation was not included, and the defect has tetrahedral symmetry. The dashed line is only a guide to the eye.

becomes very small. Increasing the cluster size from 47 to 71 atoms leads to a change of 1 mRy. The fact that the defect is positively charged and we truncate the Coulombic tail of the potential may be seen more clearly by looking at the plot of the electronic charge perturbation for the  $P^+$  impurity. In Fig. 4 we have plotted the two quantities

$$q_e(r) \equiv \int d\hat{r} \Delta n_e(r) \quad (35)$$

and

$$Q_e(r) \equiv \int_0^r dr' r'^2 q_e(r'). \quad (36)$$

$q_e$  and  $Q_e$  represent, respectively, the spherically averaged electronic density perturbation and the radially integrated charge perturbation.

From the plot of the integrated charge perturbation, it may be seen that screening is quite effective in silicon, since at a distance of approximately one bond length, i.e.,  $4.44a_0$ , from the defect, the total integrated screening charge is already very close to its asymptotic value of  $1 - 1/\epsilon_0$ , given by the dashed line in the figure. The remaining oscillations around this asymptotic value simply reflect the microscopic inhomogeneity of the unperturbed medium. Adding more shells of atoms in the self-consistent Green's-function calculation simply extends further out the effect of these small oscillations around the asymptotic (macroscopically averaged) value. From the calculated formation energy it does not seem, however, that these long-range oscillations of the charge density have any great importance.

The truncation of the long-range Coulombic tail of the

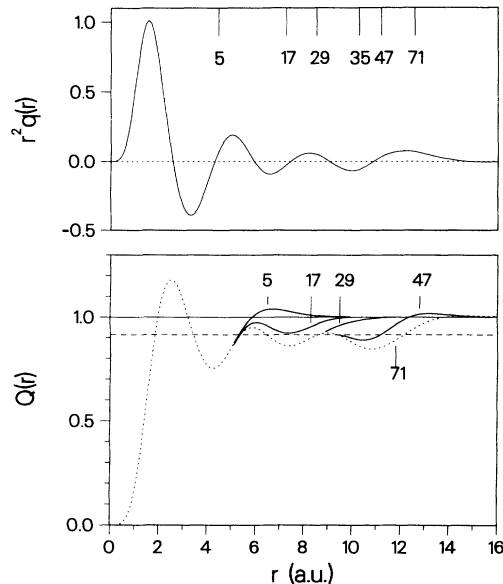


FIG. 4. Radial dependence of (a)  $r^2 q_e(r)$  calculated with a 71-atom cluster, and (b)  $Q_e(r)$  calculated for different sizes of cluster for substitutional  $P^+$  in silicon.  $q_e(r)$  and  $Q_e(r)$  are defined in Eqs. (35) and (36), respectively. The shells of atoms about the impurity are indicated on the upper horizontal axis. The dashed horizontal line in (b) indicates the asymptotic value  $1 - 1/\epsilon_0$ .

potential has also another effect; namely, for any given cluster size, the screening charge oscillates around its asymptotic value up to the outer surface of the cluster, where there is an additional charge approximately equal to  $1/\epsilon_0$ . This has the effect of minimizing the self-consistent potential that extends further outside the cluster and is truncated in the calculation. In the limit of an infinite cluster, this effect will disappear. In a finite cluster, it constitutes an unphysical size-dependent effect. However, only the outermost surface of the cluster is affected, and the net effect on the relevant physical quantities is very small.<sup>34</sup>

The existence of different charge states for a given defect provides another way of testing the numerical accuracy and internal consistency of the calculations by checking how well the relation<sup>35-37</sup>

$$\frac{\partial E}{\partial f_i} = \epsilon_i, \quad (37)$$

which is exact for local-density functionals, is satisfied. Equation (37) is the basis for the so-called Slater transition-state rule,<sup>38</sup> namely

$$\Delta E \equiv E(f_i = 1) - E(f_i = 0) \simeq \epsilon_i(f_i = \frac{1}{2}), \quad (38)$$

which is known to hold very well for atoms and molecules. Here  $E(f_i = 1$  or  $0)$  is the total energy of a many-electron system in which the occupation number of the  $i$ th single-particle (Kohn-Sham) state is equal to 1 or 0, respectively, whereas  $\epsilon_i(f_i = \frac{1}{2})$  is the  $i$ th Kohn-Sham eigenvalue when the occupancy is  $\frac{1}{2}$ .

The total energy  $E(f)$  and the eigenvalue  $\epsilon(f)$  were calculated for the charge states of the unrelaxed silicon vacancy corresponding to the occupancies  $f = \frac{1}{2}, 1, \frac{3}{2}, 2, \frac{5}{2}$ , and 3 of the  $t_2$  gap state. These calculations were performed using basis set II and including three shells of neighbors. The results of these calculations are given in Table III. Also given in the same table are the total-energy differences  $E(f + \frac{1}{2}) - E(f - \frac{1}{2})$  for comparison with the eigenvalue  $\epsilon(f)$ . As can be seen, the errors are very small ( $\sim 1$  mRy), giving a check on the internal consistency of the total-energy calculation. The largest discrepancies occur when  $\epsilon_{t_2}$  is close to the valence- or conduction-band edges, and they are related to an inaccurate determination of the position of the bound state when it is close to the continuum of band states.

The Slater transition-state rule has been frequently used to obtain the difference in total energy between two different charge states of a defect at the cost of a relatively simpler eigenvalue calculation. Eigenvalues obtained from Green's-function calculations have been used, in conjunction with the Slater transition rule, to obtain total-energy differences in defect calculations, before the development of working schemes for total energies, leading to some important results.<sup>39,40</sup> Implicit in the use of (38) is that the charge-state dependence of the local relaxation may be neglected.

#### D. Silicon self-interstitial

As an example of the use of the adspace, we first consider an unrelaxed self-interstitial  $I_T$  at the interstitial site

TABLE III. Test of the Slater transition-state rule for different charge states of the unrelaxed silicon vacancy. Energies are in Rydbergs.

$f_{t_2}$	$E(f_{t_2})$	$\epsilon_{t_2}$	$E(f_{t_2} + \frac{1}{2}) - E(f_{t_2} - \frac{1}{2})$	difference
3.0	0.4543			
2.5	0.4209	0.0614	0.0604	0.0010
2.0	0.3939	0.0486	0.0482	0.0004
1.5	0.3728	0.0374	0.0375	-0.0001
1.0	0.3564	0.0283	0.0289	-0.0006
0.5	0.3439	0.0210	0.0179	-0.0031
0.0	0.3386			

of tetrahedral symmetry. The formation energy for the doubly positively charged self-interstitial  $E_F(I_T^{2+})$ , calculated using the different basis sets listed in Table II, is shown in Fig. 5 as closed circles. The Fermi energy is assumed to be positioned at the top of the valence band. Just as in the treatment of the vacancy, the total energy was converged with respect to the range of the perturbation by adding shells of atoms around the self-interstitial. There are shells containing 5,11,23,31,43,67,83, . . . sites about the tetrahedral site. To obtain convergence in the energy of  $\sim 1$  mRy, it was necessary to use clusters of 31, 31, 31, 43, and 43 atom sites for basis sets I, II, III, IV, and V, respectively. Larger clusters were needed with the last two basis sets because of the contribution to the  $\Delta t$  and  $\Delta S$  terms in (17) arising from the long-range basis functions. In the latter case the convergence was determined by performing calculations for clusters containing 67 atoms.

From Fig. 5 it may be seen that if only  $s$  and  $p$  basis functions are considered,  $E_F(I_T^{2+})$ , which is approximately 0.39 Ry, is not very sensitive to either the number or range of these functions. Including  $d$  orbitals, however, leads to a large reduction of  $\sim 0.15$  Ry in the formation energy. This may be attributed to the inability of  $sp^3$  hybrid orbitals to describe the fivefold coordination of the nearest neighbors of the tetrahedral self-interstitial. Although the change in the energy per atom of the perfect crystal when  $d$  orbitals are included is only  $\sim 30$  mRy (see Table II), the change in the formation energy of the self-interstitial is a factor of 5 larger. Adding yet another  $d$ -orbital changes the energy of the host by  $\sim 5$  mRy per atom. Assuming the formation energy may change by as much as a factor of 5 times this amount implies a possible change in the formation energy by as much as 25 mRy. Such a calculation would take a factor  $[(14+5)/14]^3 \sim 2.5$  longer than the calculation with basis set V and was not attempted. Our best value for the formation energy of  $I_T^{2+}$  (without relaxation of the neighboring atoms) is thus 0.255 Ry.

The formation energy was also calculated for a silicon self-interstitial  $I_H$  at the hexagonal symmetry site using different basis sets. The results for the doubly positively charged state  $I_H^{2+}$ , shown in Fig. 5 as open circles, display the same sensitivity to inclusion of  $d$  orbitals as those for the tetrahedral self-interstitial. The path connecting the tetrahedral and hexagonal symmetry sites has been proposed as one possible migration path that may play a role in self-diffusion in silicon.<sup>11-13</sup> Assuming that the ener-

gies at these two sites are extrema, then the migration energy is given by the difference in formation energies at the two sites. This is given by the height of the vertical lines connecting the circles in Fig. 5. A substantial cancellation of errors occurs when we calculate this difference (Table IV), but a significant sensitivity to the inclusion of  $d$  orbitals remains. The best estimate (basis set V) for the migration energy of the doubly ionized self-interstitial, neglecting lattice relaxation, is 0.117 Ry ( $= 1.6$  eV).

At the tetrahedral interstitial site, the unoccupied  $p$  states of the  $I_T^{2+}$  form a localized triply degenerate  $\epsilon_{t_2}$  state in the upper half of the band gap. In order to form the  $I^+$  and  $I^0$  charge states, this single-particle eigenstate must be populated. As a result of the Coulomb repulsion between the electrons populating it, the position of the  $t_2$

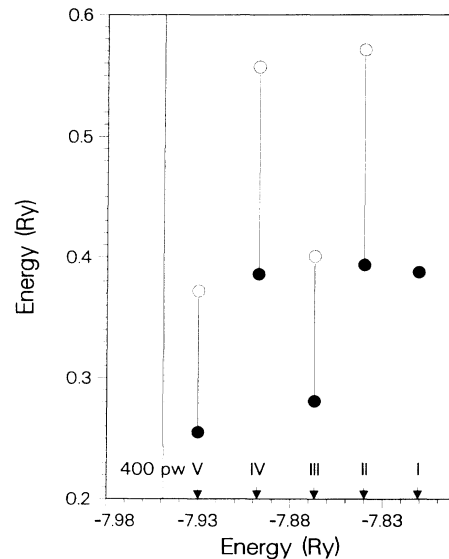


FIG. 5. Formation energy of the doubly positively charged self-interstitial at the tetrahedral (closed circles) and hexagonal (open circles) symmetry sites for the different basis sets detailed in Table II. For each basis set, the total energy was converged with respect to the cluster size to better than 1 mRy. Relaxation of the neighboring atoms is not included here. The  $x$  coordinate is the total energy per Si atom for the perfect crystal. The values calculated with the five different basis sets are indicated by arrows. For comparison, the total energy obtained for the perfect crystal with a plane-wave basis is included.

TABLE IV. Formation energy of three different charge states of the self-interstitial at tetrahedral and hexagonal sites for different basis sets, assuming the Fermi energy is placed at the top of the valence band. The difference in these energies is the migration energy. Relaxation of the lattice atoms (nearest neighbors only) is included in the last column only. Energies are in Rydbergs.

	Basis set	II	III	IV	V	V
$I^{2+}$	$E_F(I_H)$	0.570	0.401	0.557	0.372	0.324
	$E_F(I_T)$	0.394	0.281	0.386	0.255	0.234
	$E_M$	0.176	0.120	0.171	0.117	0.090
$I^+$	$E_F(I_H)$	0.570	0.401	0.557	0.372	0.324
	$E_F(I_T)$	0.459	0.342	0.440	0.304	0.290
	$E_M$	0.111	0.059	0.117	0.068	0.034
$I^0$	$E_F(I_H)$	0.578	0.401	0.557	0.372	0.324
	$E_F(I_T)$	0.548	0.406	0.503	0.355	0.348
	$E_M$	0.030	0.005	0.054	0.017	-0.024

state depends on its occupancy  $f$ ,  $\varepsilon_{i_2} = \varepsilon_{i_2}(f)$ , and it may happen that the localized state moves into the conduction band to become a resonance. In a LDA calculation problems arise because the fundamental band gap in the single-particle eigenvalue spectrum is smaller than the experimental gap, and states that should be localized instead occur as conduction-band resonances. For silicon, the calculated band gap is found to be 0.038 Ry (=0.52 eV) compared to the experimental value of 0.086 Ry (=1.17 eV). The electronic structure of the unperturbed system may be modified so as to give agreement with the experimental band gap, but a correction must then be made to the total energy.<sup>13</sup> This correction may be large, depending on the way in which the gap is modified. This approach, for which there is no formal justification, has not been adopted in this publication. All the results presented here have been obtained with an unmodified band gap and represent straightforward local-density-approximation energies.

In the case we are considering, the  $p$  state becomes a resonance in the conduction band for an occupancy of  $f=2$ . The extra electron used to form  $I_T^0$  from  $I_T^+$  occupies the lowest unoccupied state, which in this case is a delocalized effective-mass-like state. We do not attempt to calculate the position of such a state, but instead use the Slater transition-state rule (38) to derive the formation energy of  $I_T^0$  from that of  $I_T^+$ . Neglect of the charge-state dependence of the local relaxation is justifiable because of the delocalized nature of the state occupied by the extra electron. The error inherent in this procedure is of the order of the shallow-donor ionization energy,  $\sim 3$  mRy. The results of calculations performed for the formation energies of the  $I^+$  and  $I^0$  at both tetrahedral and hexagonal symmetry sites are tabulated in Table IV, together with the migration energies. The effect of including lattice relaxation will be considered in the following section.

## E. Lattice relaxation

### 1. Lattice vacancy

As our first example of the calculation of the lattice relaxation about an impurity, we consider the case of the

symmetric breathing-mode relaxation of the four atoms surrounding a silicon lattice vacancy. This problem has been examined previously.<sup>39,41-43</sup> In Ref. 39 the relaxation about a neutral lattice vacancy was not calculated, but by analogy with the Si(111) surface it was assumed to be outwards (*away* from the vacant lattice site) or towards a more planar  $sp^2$ -like bonding configuration of each of the four nearest-neighbor silicon atoms to their three remaining neighbors. Later, Lindelfelt<sup>41</sup> and Scheffler, Vigneron, and Bachelet<sup>42</sup> found an outward breathing relaxation for the  $V^0$  using their first-principles Green's-function force calculations. We have found,<sup>12,43</sup> on the contrary, an *inward* breathing relaxation. More recently, an inward breathing relaxation has also been found in repeated supercell calculations.<sup>44</sup> It is worthwhile examining the vacancy relaxation in more detail, both because of its intrinsic interest and because it serves as a test case for many first-principles calculations.

The force on the four atoms surrounding the unrelaxed vacancy, which is the slope  $dE/d\delta$  of the total-energy function, is given in a finite-difference approximation  $\Delta E/\Delta\delta$  in Fig. 6. For different cluster sizes, the energy of the unrelaxed vacancy  $E(\delta=0)$  and for a small inward displacement of the four atoms  $E(\delta=-0.1a_0)$  is shown. The results shown were calculated with basis set II. Clusters containing 17, 29, 35, 47, and 71 atoms are defined by choosing all atoms within a certain radius of the central site. This procedure assumes that the range of the perturbation is determined by the central-site contribution. If, however, the range of the perturbation is determined by the four displaced atoms, then it may be more efficient to define clusters containing all atoms within a certain radius of the four displaced atoms. This defines clusters containing 41 (all next-nearest neighbors of the displaced atoms), 59, 71, . . . atoms, which we will denote by  $41^*$ ,  $59^*$ , and  $71^*$  to distinguish them from the clusters made up of complete shells of atoms centered on the vacancy site. For a small cluster, for which the total energy is not converged, the force is outwards, corresponding to an outward breathing relaxation (away from the vacant lattice site). As the cluster size is increased, the force changes, and when the calculation is converged with respect to the cluster size, the force is, as described

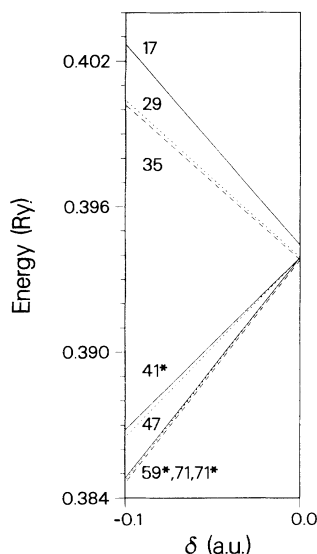


FIG. 6. Formation energy of the neutral lattice vacancy without radial relaxation ( $\delta=0$ ) and with a small inward relaxation ( $\delta=-0.1a_0$ ) of the four silicon atoms around the vacant lattice site. The slope approximates the force on the four atoms. The calculations were performed with basis set II for a number of different cluster sizes, outside of which the perturbation was truncated. The cluster sizes are explained in the text.

above, inwards. A changeover in behavior occurs for 35- and 41\*-atom clusters, which differ in that the 41\* cluster includes all of the next-nearest-neighbor atoms of the four atoms displaced in the breathing mode. Inclusion of more shells of atoms leads to only small differences, and a 59\* cluster is sufficient to calculate the breathing relaxation with mRy convergence. In all of the calculations to be discussed, the cluster size is sufficiently large that the total energy is converged to  $\sim 1$  mRy.

In Fig. 7 we show the formation energy for a neutral lattice vacancy as a function of the displacement  $\delta$  of the four atoms surrounding the central (vacant) site in a symmetric breathing mode. These results were calculated with basis set II and a 71-atom cluster both for the case where orbitals were included on the vacancy site (closed circles) and where these orbitals were omitted (open circles). Although an inward relaxation is found in both cases, there are differences in detail resulting from using a minimal basis set. In particular, the amplitude of the breathing relaxation is found to be  $0.47a_0$  and the energy gain is 0.039 Ry when the vacancy site orbitals are omitted. When they are included, the breathing relaxation is calculated to be  $0.35a_0$  and the energy gain is only 0.018 Ry. The corresponding results calculated with basis set IV, containing more extended orbitals, are shown in Fig. 8. The breathing relaxation is found to be  $\sim -0.48a_0$  both with and without orbitals on the vacant site, and the energy gain is found to be 0.034 and 0.032 Ry, respectively. The discrepancies are seen to be reduced significantly by using the improved basis. The effective force constant, given by the curvature of  $E(\delta)$ , becomes smaller as the basis set is improved. Performing a least-squares fit to a cubic polynomial in the displacement  $\delta$ , the equilibrium

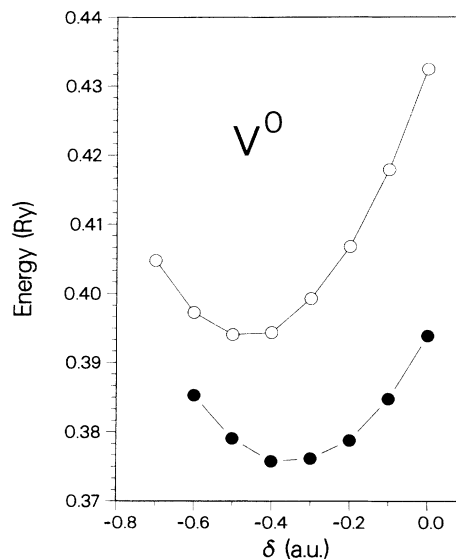


FIG. 7. Formation energy of the neutral lattice vacancy as a function of the radial relaxation  $\delta$  of the four silicon atoms around the vacant lattice site. The calculations were performed with basis set II and a cluster of 71 atoms was used to represent the perturbation. The total energy was converged with respect to the cluster size to better than 1 mRy. Calculations where the basis functions on the vacant site were removed (retained) are denoted by open (closed) circles.

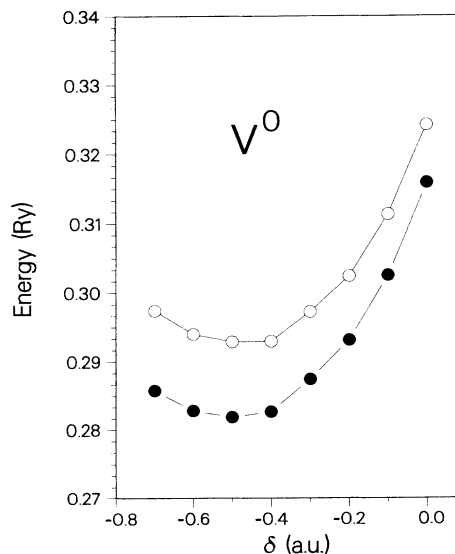


FIG. 8. Formation energy of the neutral lattice vacancy as a function of the radial relaxation  $\delta$  of the four silicon atoms around the vacant lattice site. The calculations were performed with basis set IV and a cluster of 71 atoms was used to represent the perturbation. The total energy was converged with respect to the cluster size to better than 1 mRy. Calculations where the basis functions on the vacant site were removed (retained) are denoted by open (closed) circles.

relaxation  $\delta_0$ , the energy gain  $E(0) - E(\delta_0)$ , and the force constant  $k_\delta = \frac{1}{2} d^2 E / d\delta^2 |_{\delta=\delta_0}$  are obtained. These are given in Table V for the results of the calculations with basis sets I, II, III, and IV for the neutral lattice vacancy  $V^0$ , both with orbitals included on the vacant site and without. Our best estimate of the formation energy of the neutral lattice vacancy including symmetric breathing relaxation of the nearest-neighbor atoms only is the average of 0.282 and 0.293 Ry (Table V, basis set IV) or 0.288 Ry ( $=3.9$  eV).

In addition to the symmetric breathing relaxation, the neutral lattice vacancy undergoes a symmetry-lowering, Jahn-Teller distortion. In a previous publication,<sup>43</sup> where we calculated it from first principles, we found a gain of 0.007 Ry arising from the pairing of the four silicon atoms surrounding the vacancy site. Using this latter value and the value 0.288 Ry just quoted, we find a value for  $E_F(V^0)$  of 0.281 Ry ( $=3.8$  eV).

The corresponding results for the doubly positively charged lattice vacancy are given in Table VI. The magnitude of the inward breathing relaxation is smaller for the charged state, which is consistent with the positive deformation potential  $d\varepsilon_{t_2}/d\delta|_{\delta=0}$  found for the  $t_2$  symmetry gap state in this and other LDA calculations.<sup>39,41-43</sup> We see (Table VI, basis set IV) that the formation energy of the doubly positively charged vacancy lies between 0.251 and 0.262 Ry, where the Fermi level is assumed to be pinned at the top of the valence band ( $\mu=0$ ). For the doubly positively charged vacancy there is no Jahn-Teller distortion, and we take as our best estimate for  $E_F(V^{2+})$  the average of 0.251 and 0.262 Ry or 0.257 Ry ( $=3.5$  eV). Experimentally, it is known<sup>45</sup> that, with  $\mu=0$ ,  $E_F(V^0) - E_F(V^{2+}) = 0.006$  Ry, whereas we find that  $E_F(V^0) - E_F(V^{2+}) = 0.281 - 0.257 = 0.024$  Ry.

A possible cause of this discrepancy is the neglect of long-range lattice relaxation. This may be estimated<sup>39</sup> using the Keating model.<sup>46</sup> For the doubly positively charged vacancy, the energy gain resulting from inclusion of long-range relaxation is about 0.010 Ry. Our best estimate for  $E_F(V^{2+})$  including this becomes  $0.257 - 0.010$  Ry  $= 0.247$  Ry ( $=3.4$  eV). Because the inward breathing relaxation and force constants for  $V^0$  are larger

( $\delta_0 = -0.48a_0$ ,  $k_\delta = 0.26$  Ry/ $a_0^2$ ) than for  $V^{2+}$ , the effect of the long-range relaxation is also larger; it is estimated to reduce the energy by about 0.015 Ry. Including long-range relaxation in the same simple fashion for the pairing mode increases the Jahn-Teller energy gain from 0.007 to 0.032 Ry.<sup>43</sup> Using this latter value, our best estimate for  $E_F(V^0)$  is  $0.288 - 0.015 - 0.032 = 0.241$  Ry ( $=3.3$  eV), which is now 0.006 Ry less than  $E_F(V^{2+})$ . With a slightly smaller contribution of the long-range relaxation in the Jahn-Teller energy gain, good agreement with experiment would be obtained. The energy gain calculated from first principles was only 0.007 Ry. The remaining  $0.032 - 0.007 = 0.025$  Ry, which was estimated by means of the Keating model, is more than the amount by which  $E_F(V^0)$  is lower than  $E_F(V^{2+})$ . Clearly, the distortion contributing most of the 0.025-Ry energy gain ought to be calculated from first principles. Such a calculation is at present not feasible. Using the calculated value of the formation energy of the doubly positively charged vacancy, for which there is no Jahn-Teller distortion and only a small breathing relaxation, together with the experimentally determined relation  $E_F(V^0) = E_F(V^{2+}) + 0.006$  Ry, our best estimate for  $E_F(V^0)$  is 0.263 Ry ( $=3.6$  eV).

The best value of the force constant  $k_\delta$  for a breathing relaxation of the neutral vacancy is (Table V, basis set IV)  $0.26$  Ry/ $a_0^2 = 12.6$  eV/ $\text{\AA}^2$ . This value is obtained by including nearest-neighbor relaxation only and is 70% larger than the value of  $7.5$  eV/ $\text{\AA}^2$  estimated in Ref. 39. When long-range relaxation is included using a Keating model and the parameters of Ref. 39, a value close to  $=7.5$  eV/ $\text{\AA}^2$  is found.

## 2. Self-interstitial

In the previous section, the migration energy  $E_M$  of a self-interstitial along a path where the tetrahedral and hexagonal sites are assumed to correspond to extrema in the energy was calculated to be 0.117 Ry for  $I^{2+}$ , 0.068 Ry for  $I^+$ , and 0.017 Ry for  $I^0$  (Table IV, basis set V). No account was taken of the lattice relaxation in these calculations. However, the distance from the self-

TABLE V. Parameters characterizing the relaxation of the four atoms surrounding the neutral lattice vacancy for four different basis sets. The unrelaxed energy,  $E(0)$ , for basis set V is included for reference. Energies are in Rydbergs. (To obtain the force constants appropriate to normal-mode amplitudes,  $k_\delta$  must be divided by 4.)

	Basis set	$\delta_0(a_0)$	$E(0)$	$E(\delta_0)$	$E(0) - E(\delta_0)$	$k_\delta$ (Ry/ $a_0^2$ )
No orbitals on central vacant site	I	-0.23	0.466	0.453	0.013	0.46
	II	-0.47	0.432	0.394	0.039	0.39
	III	-0.54	0.366	0.314	0.052	0.38
	IV	-0.47	0.324	0.293	0.032	0.26
	V		0.326			
Including orbitals on central vacant site	I	-0.12	0.424	0.421	0.003	0.42
	II	-0.35	0.394	0.376	0.018	0.30
	III	-0.52	0.332	0.299	0.033	0.27
	IV	-0.49	0.316	0.282	0.034	0.26
	V		0.319			

TABLE VI. Parameters characterizing the relaxation of the four atoms surrounding the doubly positively charged lattice vacancy for three different basis sets. The Fermi energy is assumed to lie at the top of the valence band. Energies are in Rydbergs.

	Basis set	$\delta_0(a_0)$	$E(0)$	$E(\delta_0)$	$E(0) - E(\delta_0)$	$k_\delta$ (Ry/ $a_0^3$ )
No orbitals on central vacant site	I	-0.15	0.415	0.411	0.004	0.37
	II	-0.40	0.391	0.366	0.025	0.23
	IV	-0.37	0.280	0.262	0.018	0.14
Including orbitals on central vacant site	I	0.02	0.365	0.365	0.000	0.34
	II	-0.21	0.344	0.339	0.005	0.23
	IV	-0.43	0.271	0.251	0.020	0.18

interstitial at the hexagonal symmetry site to its nearest neighbors is only  $4.25a_0$ . This is less than the equilibrium Si-Si separation of  $4.44a_0$ , so that we expect a significant relaxation of the surrounding silicon atoms. Using basis set II, the symmetric breathing relaxation of the six nearest-neighbor atoms is found to reduce the formation energy by 0.056 Ry, and the displacement of the neighboring atoms is  $0.18a_0$ , leading to an equilibrium Si-Si separation of  $4.43a_0$ . This calculation was performed with a cluster containing 65 atoms about the interstitial site. The energy gain decreases from 0.105 to 0.059 to 0.056 Ry on increasing the number of atoms in the cluster from 39 to 53 to 65, respectively. Including  $d$  orbitals (basis set III) and using a cluster containing 53 atoms leads to a symmetric breathing relaxation of  $0.19a_0$  and a smaller energy gain of 0.048 Ry. This relaxation is taken into account in the last column of Table IV, where the formation energy calculated with basis set V is corrected with the relaxation energy calculated with basis set III.

For the self-interstitial at the tetrahedral symmetry site with a deep level in the gap, we find a charge-state-dependent radial relaxation of its four nearest neighbors. The resulting energy gain is calculated to be 0.021 Ry for  $I_T^{2+}$ , 0.014 Ry for  $I_T^+$ , and 0.007 Ry for  $I_T^0$  using basis set II and a 43-atom cluster. The cluster size was checked by using a 67-atom cluster. The corresponding displacements of the nearest neighbors are 0.15, 0.13, and  $0.10a_0$ , respectively. The formation energies calculated with basis set V corrected with the relaxation energy calculated using basis set II are also given in the last column of Table IV. The effect of long-range relaxation is not included in these results.

#### F. Migration energy of interstitial oxygen

So far we have been concerned with quantities that have not been measured directly. In this section we will calculate the energy required for interstitial oxygen ( $O_I$ ) to hop from one bond-bridging site to an adjacent bond-bridging site (Fig. 9). This energy has been measured by stress-induced dichroism to be 2.56 eV (Ref. 47) and the high-temperature diffusion of oxygen in silicon has been successfully interpreted in terms of this mechanism.<sup>48</sup> Because the oxygen  $2s$  and  $2p$  states are so much more localized than the valence states of silicon, and because there is a large lattice distortion associated with intersti-

tial oxygen, defect calculations for oxygen in silicon present considerable technical difficulties. Unlike the examples we have considered so far, oxygen does not have a weak pseudopotential. However, a norm-conserving pseudopotential can still be defined for the valence states of oxygen,<sup>17</sup> and the pseudopotential parameters we use are given in Table I. Minimizing the total energy for the free oxygen atom with respect to the orbital exponents  $\gamma_{nl}$  of a  $3 \times s$ ,  $3 \times p$  Gaussian-orbital basis resulted in the set of exponents  $\gamma_s = (0.20, 0.75, 5.60)$  and  $\gamma_p = (0.20, 0.85, 4.00)$ . The smallest allowed exponent was  $\gamma_l = 0.20$ . In our study of the Si self-interstitial, we saw that the choice of  $s$  and  $p$  orbital exponents was not critical, but that it was important to include  $d$  orbitals on the host atoms. The calculations to be discussed below were therefore carried out with host basis sets II and III. The electronic relaxation was calculated on as many sites as were necessary to converge the total energy to better

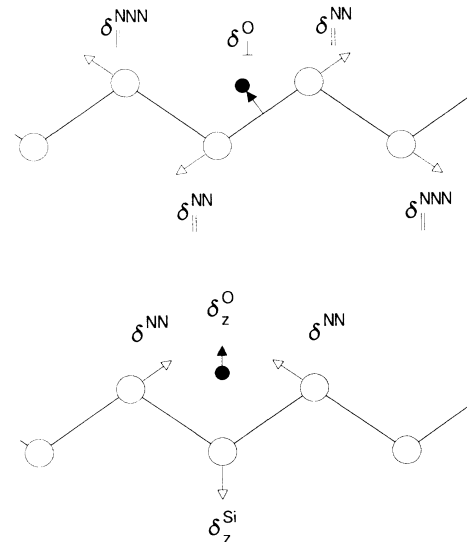


FIG. 9. Sketch of the configurations used in the calculation of the activation energy for diffusion of an interstitial oxygen atom in a silicon host crystal showing the equilibrium (upper panel) and saddle-point (lower panel) configurations. The large open circles represent a chain of silicon atoms in the (110) plane, and the small closed circle represents the oxygen atom. The displacements that are indicated by arrows are discussed in the text.

than 1 mRy. Because of the large lattice distortion induced by interstitial oxygen, up to 80 sites were included in the calculations to demonstrate convergence. The size of the defect cluster and the volume where the charge density deviates significantly from that of the perfect crystal determine the size of the cube on which the perturbed charge density and defect potential had to be calculated. A regular real-space mesh was initially used to perform numerical integrations over the cube involving the silicon host and the (localized) oxygen-defect pseudowave functions. The size of this cube (volume= $L^3$ ) and the real-space mesh interval  $l=0.26a_0$  were chosen so as to obtain convergence of the total energy to better than 1 mRy. The total number of points used was  $(L/l)^3=(120)^3$ . The most time consuming steps in the calculation were (i) the solution of the Dyson equation (19) by matrix inversion, (ii) the calculation of the charge density (15), and (iii) the calculation of matrix elements of the perturbing potential (16). In all these steps, full use was made of symmetry to reduce the computation to a minimum. Steps (ii) and (iii) required almost an order of magnitude more computer time than in the calculations discussed previously because the mesh required to obtain comparable accuracy was a factor  $(\frac{5}{2})^3$  more dense.

In order to improve the efficiency of the calculation, a "double-mesh" scheme for representing fast and slowly varying charge densities, solving the Poisson equation, and calculating matrix elements of the Hartree and exchange-correlation potentials, was implemented. In this scheme, a dense inner mesh extending over a limited region of space about the oxygen atom is used to describe the rapidly varying oxygen charge density. This inner mesh is commensurate with a coarser outer mesh that extends over the full volume of the defect cluster. This scheme was tested by (i) displacing a single silicon atom with this double-mesh scheme and comparing the results to those obtained with a single mesh. Because only the central atom was displaced, the defect cluster was small. (ii) Calculations were carried out for the symmetric breathing mode about a silicon lattice vacancy with the double-mesh scheme and compared to the results of calculations where a single mesh was used. (iii) Calculations were performed for high-symmetry configurations involving oxygen with the double-mesh scheme and compared with the results obtained with a uniformly dense mesh. Because of the high symmetry and the short range of the perturbation, very dense meshes could be tested. The density of the inner mesh was chosen so that the difference in the absolute total energy of a substitutional oxygen atom calculated with the double mesh and with a uniform dense mesh was less than 1 mRy. The calculation of the charge density and matrix elements is still very costly when the symmetry is low. An alternative scheme for solving the Poisson equation when the charge density can be decomposed into fast and slowly varying parts has been described in great detail by Feibelman.<sup>49</sup>

The accepted model for  $O_1$  is that the oxygen atom interrupts a normal Si—Si bond, as shown schematically in Fig. 9. Assuming that the saddle-point configuration for bond switching is as shown in the figure, evaluation of the activation energy requires finding the energy minimum

for each configuration. The equilibrium configuration of  $O_1$  has only  $C_{1h}$  symmetry, while the assumed saddle-point configuration has  $C_{2v}$  symmetry. Because of these low symmetries, no attempt was made to minimize the energy simultaneously with respect to all the degrees of freedom compatible with the given symmetry. To study the equilibrium configuration, the energy was first minimized with respect to  $\delta_1^O$  as a function  $\delta_{\parallel}^{NN}$ , keeping  $\delta_{\parallel}^{NNN}=0$ .  $\delta_1^O$  is the magnitude of the displacement of the oxygen atom from the bond-center site, perpendicular to the bond (maintaining  $C_{1h}$  symmetry).  $\delta_{\parallel}^{NN}$  and  $\delta_{\parallel}^{NNN}$  are the displacements of the oxygen-atom's nearest-neighbor and next-nearest-neighbor silicon atoms along the bond directions. These displacements are indicated in Fig. 9. In a second step, the energy was minimized with respect to  $\delta_{\parallel}^{NNN}$ , again as a function of  $\delta_{\parallel}^{NN}$ , but this time keeping  $\delta_1^O=0$ . Long-range relaxation, which was included in this second step by means of a Keating model using the parameters given in Ref. 39, resulted in an energy gain of less than 0.1 eV. Finally, the energy was minimized with respect to  $\delta_{\parallel}^{NN}$ , assuming that the energy gained by relaxation with respect to  $\delta_1^O$  and  $\delta_{\parallel}^{NNN}$  is additive. The calculated displacement of the nearest-neighbor Si atoms at this minimum was  $0.95a_0$ , of the second-nearest-neighbor Si atoms,  $0.20a_0$ , and of the oxygen atom,  $\delta_1^O$ ,  $1.15a_0$ . The resulting Si—O bond length is  $3.35a_0$ , which is about 10% larger than typical Si—O bond lengths found<sup>50</sup> in  $SiO_2$ . The calculated Si—O—Si bond angle is  $140^\circ$ . At the calculated minimum there are no energy levels in the gap and the defect is electrically neutral.

The total energy corresponding to the saddle-point configuration is minimized in a similar manner. The calculated displacement  $\delta_2^{Si}$  of the silicon atom on the (001) axis from its lattice site is  $0.30a_0$ , and the Si-O separation is  $3.80a_0$ . The separation to the two other neighboring Si atoms is slightly smaller,  $3.65a_0$ . The saddle-point configuration has no donorlike gap states. However, it does have a deep *acceptor* level originating in the incomplete oxygen  $2p$  shell at  $\sim E_v + 0.2$  eV.

These calculations were performed without  $d$  orbitals on the host atoms (basis set I), and the resulting difference in energies between the neutral ground state and saddle-point configurations is 2.2 eV.<sup>51</sup> Repeating the calculations with basis set III resulted in an activation energy of 2.5 eV. The only significant change in the bonding is that for the saddle-point configuration, the Si—O separation along the (001) axis is reduced to  $3.55a_0$ . In view of the spread of results found for energy differences with different basis sets when the neighboring atoms of the vacancy (Tables V and VI) and the self-interstitial (Table IV) are allowed to relax, the near-perfect agreement with the experimental activation energy of oxygen must be regarded as fortuitous. However, in the absence of a large discrepancy with experiment and because of the relatively small sensitivity to inclusion of  $d$  orbitals (2.2 versus 2.5 eV), we conclude that calculations with minimal basis sets can provide useful information about equilibrium geometries and electronic properties of oxygen-related defects in silicon. The efficiency of the search for equilibrium geometries of low-symmetry

configurations can be improved by calculating the forces acting on the atoms.<sup>29</sup>

#### IV. DISCUSSION

The Green's-matrix method was introduced in order to solve several problems encountered when attempts were made to calculate defect total energies using the conventional Green's-operator method.<sup>10</sup> In one respect, the method has been successful: the problems relating to the unbound spectrum of the Green's operator, to representing accurately the perturbation introduced when atoms are displaced and, to introducing orbitals that are unnecessary in the host crystal (such as the extra orbitals needed to describe a self-interstitial or the  $d$  states of a substitutional transition-metal atom in an  $sp$  host material) are resolved quite simply. All the Green's-function calculations of total energies that have been reported have either been carried out with the original Green's-matrix<sup>12, 13, 43, 51–54</sup> or related methods<sup>27, 55–57</sup> and not with Green's-operator methods. In this paper we have shown that *absolute* values of the formation energies of lattice vacancies and self-interstitials in a silicon host lattice may be calculated with reasonable accuracy with a quite modest basis set of only 14 orbitals per atom (basis set V). The major shortcoming of the matrix method is that the perturbation consists not only of a real physical perturbation (16), but also of a component whose range depends on the choice of basis set. Although basis set V comprises only 14 orbitals per atom, the number of atoms that must be included explicitly in the subspace  $A$  (18) in order to obtain satisfactory convergence may be very large. To demonstrate the convergence of the total energy when the four atoms neighboring a lattice vacancy are relaxed, the subspace  $A$  would consist of a 71-atom cluster. The corresponding dimension of the matrices involved in solving the Dyson equation (19) are  $71 \times 14$ . When the symmetry of the relaxation is low this becomes prohibitive, and even for a symmetry-conserving relaxation the calculation would be very time consuming.

Simultaneously, with the introduction of Green's-function methods to calculate defect energies, first-principles repeated supercell calculations were also applied to the same problem.<sup>11, 58</sup> Since then, this method has been applied with considerable success to a large number of defects in semiconductors (see Refs. 44 and 59–63 for a representative number of examples). One of the reasons for this is the technical simplicity of band-structure calculations with a plane-wave basis.<sup>64</sup> Another important reason is that the basis can be improved systematically. However, the most important advantage of using a plane-wave basis is that total-energy *differences* can be calculated reliably long before absolute convergence has been achieved. This property was exploited to calculate the phase diagram of Si (Ref. 65) and in numerous subsequent applications. Recently<sup>66</sup> it has been demonstrated in detail for the case of hydrogen impurities in silicon.

##### A. Comparison with previous work

###### 1. Lattice vacancy

The silicon lattice vacancy has probably been studied theoretically in more detail than any other defect in a

semiconductor. Because of the large number of such studies, we will restrict ourselves here to discussing recent work that has focused on the formation energy of the lattice vacancy. Interest in this energy derives from its importance for understanding the mechanisms responsible for diffusion in silicon. The activation energy  $Q$  for self-diffusion in silicon appears to be between 4.0 and 5.0 eV, with lower activation energies being observed at low temperatures and higher energies at high temperatures.<sup>67</sup> Early on, the migration energy for the lattice vacancy was established by experiment<sup>68</sup> to be between 0.18 and 0.45 eV (depending on the charge state). With  $Q = E_F + E_M$ , we obtain a value for  $E_F$  between 3.7 and 4.7 eV. Recent positron-annihilation experiments support the lower value.<sup>69</sup>

In their first published report of calculated activation energies for self-diffusion, Car *et al.* quoted a formation energy of  $E_F(V^0) = 5.0$  eV.<sup>12</sup> This value was calculated using basis set I including orbitals on the central vacant site (Table V). In later calculations with an improved basis set a formation energy of  $\sim 3.8$  eV was found.<sup>43, 52, 54</sup> In the present calculations, the formation energy of the unrelaxed neutral lattice vacancy appears to be well converged with respect to the basis set at a value of 4.4 eV (see Fig. 2 and Table V). Including only nearest-neighbor relaxation, we find (Sec. III E) a formation energy of  $E_F(V^0) = 3.8$  eV. The largest uncertainty arises in accounting for the long-range relaxation accompanying the Jahn-Teller distortion of the neutral vacancy, and this uncertainty could be reduced by calculating the relaxation of next-nearest-neighbor atoms from first principles. However, this is not at present feasible with the Green's-matrix method. Combining the experimental value<sup>45</sup> of  $E_F(V^0) - E_F(V^{2+}) = 0.084$  eV with a value for  $E_F(V^{2+})$  of between 3.4 and 3.5 eV (depending on whether long-range relaxation is included or not), we obtain a best estimate for  $E_F(V^0)$  of between 3.5 and 3.6 eV. The relaxation energy is thus  $\sim 0.8$  eV.

The only other first-principles calculations of vacancy-formation energies we are aware of were carried out using supercell techniques combined with plane-wave basis sets. Bar-Yam and Joannopoulos<sup>58</sup> quote a relaxed formation energy for  $V^{2+}$  of  $3.7 - 0.33 = 3.4$  eV when the Fermi energy is placed at the top of the valence band. From their Table II, this value seems to be well converged with respect to the size of supercell. It compares remarkably well with our value of 3.5 eV (Table VI, basis set IV), which is obtained with an inward breathing relaxation that lowers the energy by 0.25 eV. These authors unfortunately give no detail of their calculated relaxation. Their value for  $E_F(V^0)$  was derived by combining their calculated value for  $E_F(V^{2+})$  with the experimental value of  $E_F(V^0) - E_F(V^{2+})$ , and their resulting value of  $E_F(V^0) = 3.6$  eV is therefore in good agreement with the values we have quoted above.

Antonelli and Bernholc have also calculated the neutral vacancy-formation energy using a supercell technique together with a plane-wave basis.<sup>44</sup> They find a value of  $E_F(V^0) = 4.4$  eV. Although they calculate an inward breathing relaxation that is in qualitative agreement with our findings, these authors do not quote the associ-

ated energy gain, and it is not clear whether their 4.4-eV formation energy includes radial relaxation or not.<sup>70</sup> Nichols, van de Walle, and Pantelides<sup>71</sup> have reported a formation energy of 3.5 eV for the neutral lattice vacancy calculated with the same method. It is not clear whether relaxation or Jahn-Teller distortion were taken account of, and, if so, whether they were calculated from first principles or extracted from experiment. We discussed earlier the discrepancy between our finding of an inward breathing relaxation about the lattice vacancy and the opposite finding by Lindefelt<sup>41</sup> and Scheffler, Vigneron, and Bachelet.<sup>42</sup> In view of Fig. 6, it is clear that a force calculation based on clusters of 35 atoms or fewer can easily be misinterpreted in favor of an outward breathing relaxation.

We conclude that the formation energy of the relaxed doubly positively charged vacancy is  $\sim 3.5$  eV. The formation energy of the neutral lattice vacancy is more problematic because of the difficulty of treating the Jahn-Teller distortion in an adequate fashion. By combining  $E_F(V^{2+})$  with experimental information, we arrive at a best value for  $E_F(V^0)$  of 3.6 eV. Combining this with the experimental migration energy<sup>68</sup> results in an activation energy for diffusion of 4.0 eV.

## 2. Self-interstitial

The formation and migration energies of the self-interstitial are central to an understanding of its role in self-diffusion. Unlike the vacancy, the silicon self-interstitial has not been observed directly experimentally, and there is considerable disagreement about how the activation energy  $Q$  should be divided into formation and migration energies. In the following discussion we will restrict ourselves to considering self-interstitials in the empty channels of the silicon lattice at positions of tetrahedral or hexagonal symmetry, although, as pointed out in Ref. 12, in order to mediate self-diffusion, the self-interstitial must interchange with a lattice atom.

The calculations for the self-interstitial reported in Ref. 12 were performed with basis set I augmented with  $d$  orbitals (with an unoptimized exponent  $\gamma_d$ ), which resulted in a formation energy of  $E_F(I_T^{2+})=4.9$  eV with the Fermi level placed at the top of the valence band, and  $E_F(I_H^0)=6.3$  eV. Improvement of the basis set led to reduced values of  $E_F(I_T^{2+})=3.8$  eV and  $E_F(I_H^0)=5.2$  eV.<sup>54</sup> Further improvement of the basis set and numerical procedures result in values of  $E_F(I_T^{2+})=3.2$  eV and  $E_F(I_H^0)=4.4$  eV (Table IV, last column). The dependence of these formation energies (as well as that of the other charge states given in the last column of Table IV) on the Fermi level is shown in Fig. 10. The important qualitative conclusions drawn in Ref. [12] remain true: the self-interstitial displays negative- $U$  behavior;<sup>12</sup> the electronic structure supports athermal migration in the empty channels;<sup>11,12</sup> at high temperatures where the Fermi level is positioned in the middle of the gap, the minimum formation energy for a self-interstitial of 4.4 eV is much larger than its migration energy of  $\sim 0.3$  eV and about 1 eV larger than the vacancy-formation energy (3.5 eV).

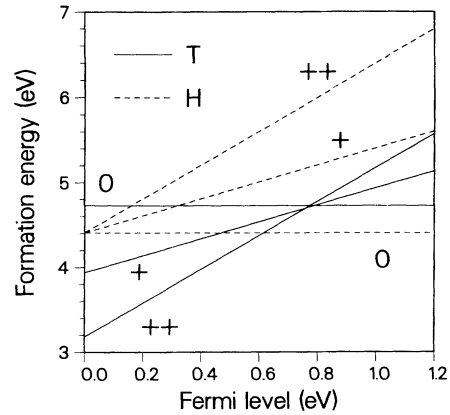


FIG. 10. Formation energy of various charge states of the self-interstitial at tetrahedral and hexagonal symmetry sites as a function of the Fermi-level position in the gap. For the Fermi level at the top of the valence band, the energies are taken from the last column of Table IV.

Green's-function calculations for the Si self-interstitial have been reported by Baraff and Schlüter.<sup>13</sup> For the formation energy  $E_F(I_T^{2+})$  with the Fermi level in the middle of the gap, they found a value of  $4.7 \pm 0.5$  eV, in agreement with our value of 4.4 eV (Fig. 10). They find a value of  $E_M(I^{2+})=1.2 \pm 0.5$  eV without relaxation and  $E_M(I^{2+})=0.4 \pm 0.4$  eV with relaxation, compared to our values of 1.6 and 1.2 eV, respectively (see Table VII). The latter value of 1.2 eV will be reduced somewhat by including long-range relaxation. Nevertheless, the agreement is only moderate. Baraff and Schlüter used clusters containing 27 sites for the tetrahedral interstitial calculation and only 19 sites for the hexagonal interstitial calculations. We saw in Sec. III E that these cluster sizes are quite inadequate for calculating the "change-of-basis" perturbation, and indeed we find that the unrelaxed hexagonal site interstitial is not converged with such a small cluster. For the neutral self-interstitial they find a value of  $E_M(I^0)=-1.1 \pm 0.5$  eV without relaxation and  $E_M(I^0)=-1.6 \pm 0.5$  eV with relaxation, compared to our values of 0.2 and  $-0.3$ , respectively. In the absence of more details, we attribute the discrepancies in large part to a lack of convergence with respect to the cluster size in

TABLE VII. Migration energy,  $E_M(I)=E_F(I_H)-E_F(I_T)$ , of two charge states of the silicon self-interstitial, with and without relaxation. The entries labeled "this work" are taken from the last two columns of Table IV. The values in parentheses are calculated by estimating  $E_F(I_T^0)$  as  $E_F(I_T^{2+})+2E_g$ , where  $E_g$  is the experimental band gap equal to 1.17 eV. Energies are in electron volts.

	Unrelaxed	Relaxed	Reference
$E_M(I^{2+})$	$1.2 \pm 0.5$	$0.4 \pm 0.5$	13
	$1.9 \pm 0.1$	$1.2 \pm 0.2$	58
	1.6	1.2	This work
$E_M(I^0)$	$-1.1 \pm 0.5$	$-1.6 \pm 0.5$	13
	$-0.5 \pm 0.3$	$-1.2 \pm 0.3$	58
	0.2 (-0.6)	$-0.3 (-1.1)$	This work

their calculation.

The migration energies for the self-interstitial calculated by Bar-Yam and Joannopoulos using a supercell method<sup>11,58</sup> are also given in Table VII. Our values for the migration energy of  $I^{2+}$  are in reasonable agreement. For the neutral self-interstitial, the large apparent discrepancy is almost entirely removed if, following the same procedure as used by those authors, we calculate  $E_F(I_T^0)$  as  $E_F(I_T^{2+}) + 2E_g$ , where  $E_g = 1.17$  eV is the experimental energy gap for silicon. The values thus calculated are shown in parentheses in Table VII. The relaxation energies found by these authors<sup>58</sup> are roughly the same as those considered in Sec. III E. For the hexagonal self-interstitial, they considered in addition to the symmetric breathing relaxation a ring-buckling relaxation. The total-energy gain from relaxation was 0.9 eV, compared to our value of 0.65 eV. This latter value would be increased if we took account of the ring-buckling and long-range relaxation. For the formation energy  $E_F(I_T^{2+})$ , Bar-Yam and Joannopoulos obtain a value of 4.0 eV, assuming the Fermi level is positioned in the middle of the (experimental) gap. This should be compared to our value of 4.4 eV (Fig. 10) and the value of 4.7 eV found by Baraff and Schlüter.<sup>13</sup> These values of  $E_F(I_T^{2+})$  are collected for comparison in Table VIII.

Antonelli and Bernholc<sup>44</sup> have also reported formation energies for self-interstitials based on plane-wave supercell calculations. They quote a formation energy of  $E_F(I_T^{2+}) = 3.6$  eV, to be compared to our best value of 4.4 eV (Table VIII). For  $E_F(I_T^0)$  they find a value of 4.3 eV, compared to our value of 4.7 eV. Nichols, van de Walle, and Pantelides<sup>71</sup> find a formation energy of 3.6 eV for a neutral self-interstitial at the tetrahedral symmetry site<sup>72</sup> using the same supercell method.

The large spread in self-interstitial formation energies<sup>58,44,70,71</sup> calculated using the plane-wave supercell method is surprising, and the source of the discrepancies is unclear. For neutral defects with no gap states, the supercell method should present relatively few problems, since the supercell size ought not to be critical, and convergence with respect to the kinetic energy cutoff (number of plane waves) and Brillouin-zone sampling should be straightforward. For neutral defects with partly filled gap states or for charged defects, the issue of supercell size is more delicate. A gap state acquires a finite dispersion, which may be considerable for typical supercell sizes. For example, van de Walle *et al.* find a gap state with a dispersion of 0.5 eV (the local-density band gap is 0.52 eV) with a 32-atom supercell for H-related defects in

Si.<sup>66</sup> To perform supercell calculations for charged defects, a neutralizing background charge must be used to avoid divergence of the electrostatic energy, and again the supercell size must be chosen sufficiently large so as to make the effect of this artificial construction negligible. In both cases, where large supercells must be used, it then becomes difficult to demonstrate convergence with respect to kinetic-energy cutoff and the Brillouin-zone sampling. It would clearly be useful if more details of the calculations for the self-interstitial were available in order to know where the difficulties lie.

The Green's-function approach does not suffer from these problems, and the largest source of uncertainty relates to the choice of basis set. A problem common to both approaches is the underestimation by the local-density approximation of the band gap. This may be important when comparing calculated results with experiment, but may be neglected for the purpose of comparing different calculations. It is, however, important to know what gap was used when the Fermi-level dependence of formation energies is being discussed or when the Slater transition-state rule (Sec. III C) is used.

### 3. Interstitial oxygen

Almost all of the theoretical studies of interstitial oxygen in silicon we are aware of have been based on cluster calculations. Most of these cluster calculations were performed using semiempirical Hartree-Fock based methods such as complete neglect of differential overlap (CNDO), modified neglect of differential overlap (MNDO), modified intermediate neglect of differential overlap (MINDO/3), etc. The difficulties associated with these methods are well known and we will refrain from attempting yet another evaluation of such calculations. In this section, we will restrict ourselves to discussing first-principles calculations where there are no free parameters.

It will be most instructive to start by comparing our results with those of a recent local-density cluster calculation by Saito and Oshiyama.<sup>73</sup> These authors have calculated the migration energy for an oxygen interstitial along the same lines as in Sec. III F, using norm-conserving pseudopotentials and Gaussian-orbital basis sets. The equilibrium configuration is studied by means of a  $\text{Si}_{10}\text{O}$  cluster (plus 20 hydrogen atoms to terminate the cluster) and the saddle-point configuration by means of a  $\text{Si}_{11}\text{O}$  cluster (plus 24 hydrogen atoms). For the equilibrium configuration, only the nearest-neighbor silicon atoms are allowed to relax, and they find a Si—O bond length of  $3.2a_0$  compared to our value of  $3.35a_0$  and a Si—O—Si bond angle of  $152^\circ$ , compared to our value of  $140^\circ$ . In their calculation, the displacement of the neighboring silicon atoms ( $\delta_{\parallel}^{\text{NN}}$  in Fig. 9) is  $0.85a_0$ , compared to our finding of  $0.95a_0$ . The smaller bond lengths they find may be a result of not allowing the next-nearest-neighbor silicon atoms to relax.

To examine the saddle-point configuration Saito and Oshiyama allow the same displacements as shown in Fig. 9. They find a large displacement of the silicon atom on the (001) axis,  $\delta_2^{\text{Si}} = 0.77a_0$ , compared to our value of  $0.30a_0$ . The distance from this silicon atom to the oxy-

TABLE VIII. Comparison of formation energies  $E_F(I_T^{2+})$  from a number of calculations where the Fermi level is assumed to be in the middle of the experimental gap. Energies are in electron volts.

$E_F(I_T^{2+})$	Reference
4.7±0.5	13
4.4	This work (Fig. 10)
4.0	58
3.6	44

gen atom in their calculation is  $3.29a_0$ , compared to our value of  $3.80a_0$ . There is thus a substantial rebonding of the saddle-point configuration in the cluster calculation compared to the Green's-function approach. Their calculated migration energy is only 1.2 eV, compared to the experimental value of 2.56 eV and our calculated value of 2.5 eV. These authors attribute part of the discrepancy to neglect of next-nearest-neighbor and long-range relaxation for the equilibrium configuration. This is confirmed in our calculation, where we find that this lowers the energy by  $\sim 0.55$  eV. Another difference between the two calculations is that we have examined the effect of including  $d$  orbitals on the host silicon atoms. This led to an increase in the migration energy of 0.3 eV and would presumably lead to a comparable increase if they were included by Saito and Oshiyama. Finally, there is the question of whether the cluster size is sufficiently large to describe the electronic states, and in particular the host semiconductor, adequately. In our calculation this is done automatically by using a Green's function for a perfect crystal and then choosing a sufficiently large cluster on which to represent this Green's function. This was done in a systematic fashion by increasing the cluster size until the total energy was converged to better than 1 mRy. In a cluster calculation a parallel procedure ought to be followed, but this was not done in Ref. 73. At this stage we must attribute the remaining discrepancy between our calculation and theirs to their use of an inadequate cluster size. One way of seeing how well the cluster simulates the perfect crystal is by looking at how well the eigenvalue spectrum of the crystal is represented in the cluster calculation. For silicon, it is well known that the local-density approximation results in a band gap of  $\sim 0.5$  eV. In a calculation for a crystal fragment containing 11 silicon atoms (plus 24 hydrogen atoms), Saito and Oshiyama find a band gap of 4.9 eV, i.e., almost an order of magnitude too large. Thus a cluster containing this number of atoms might be expected to have fundamentally different screening properties and lead to different bonding configurations than in a real silicon crystal.

Similar cluster calculations have been carried out by Snyder and Corbett<sup>74</sup> within the Hartree-Fock approximation. Using even smaller clusters than Saito and Oshiyama ( $\text{Si}_5\text{O}$  plus 12 hydrogen atoms for both equilibrium and saddle-point configurations), they calculated a migration energy of 2.84 eV. More recently, the inadequacy of these small cluster sizes has been recognized by these authors.<sup>75</sup>

## V. CONCLUSIONS

We have seen that, although the Green's-matrix method solves the problems it was designed to solve, it does so at the expense of introducing another problem,

which we have termed the "change-of-basis perturbation." This artifact of the matrix method makes it impossible to consider the relaxation of more than approximately ten atoms. For the oxygen interstitial atom it was sufficient to be able to consider the relaxation of the two nearest-neighbor and six next-nearest-neighbor host atoms for the equilibrium configuration. The remaining energy gain from long-range relaxation ( $< 0.1$  eV) was not critical to the description of the defect energetics. For the case of the neutral silicon lattice vacancy, the energy gain from relaxing the next-nearest neighbors of the vacancy site was estimated to be so large that it ought to be calculated from first principles. Because of the "change-of-basis perturbation," a reasonable calculation for such a large cluster is not possible, and the interesting problem of the negative- $U$  behavior of the silicon vacancy unfortunately cannot be addressed by means of this first-principles total-energy method. This problem also cannot be addressed at present by the alternative supercell method because the dispersion of the gap state is so large for the size of supercells for which calculations can be performed.

By performing calculations with different basis sets, we have examined in detail the issue of convergence with respect to cluster size for several different examples. The main problem with using a basis of localized orbitals is that a systematic improvement of the basis is not possible—a well-known unresolved problem in quantum chemistry. Thus, although it is plausible that our formation energies for native defects, neglecting relaxation, are converged to about 0.1 eV using basis set V, it is not possible to establish rigorous error bars. A positive point is that, in all the cases we have examined, the relaxation is described qualitatively correctly even with the worst basis set employed, so that such basis sets can be used to calculate equilibrium geometries, and more sensitive quantities can then be calculated using a better basis set.

A comparison with calculations performed using the supercell method is inconclusive because in these calculations it is frequently not stated whether the formation and migration energies reported were calculated including lattice relaxation, or if relaxation is included, whether it was calculated from first principles or derived from experiment, where the Fermi level was assumed to lie, etc. In particular, for the self-interstitial at the tetrahedral site where lattice relaxation is minimal but the discrepancies between different calculations are still very large, it would be very useful if more details of the calculations were made available.

## ACKNOWLEDGMENTS

We have benefited from numerous discussions with S. T. Pantelides, A. Oshiyama, and A. R. Williams.

<sup>1</sup>P. C. Hohenberg and W. Kohn, Phys. Rev. **136**, B864 (1964).

<sup>2</sup>W. Kohn and L. J. Sham, Phys. Rev. **140**, A1133 (1965).

<sup>3</sup>For a number of review articles, see *Theory of the Inhomogeneous Electron Gas*, edited by N. H. March and S. Lundqvist (Plenum, New York, 1983). For applications of the local-density formalism to atoms, molecules, and solids, see espe-

cially the article by A. R. Williams and U. von Barth. For a more recent review of the local-density approximation, see O. Gunnarsson and R. O. Jones, Rev. Mod. Phys. **61**, 689 (1989).

<sup>4</sup>For a review on defects in semiconductors, see *Deep Centers in Semiconductors*, edited by S. T. Pantelides (Gordon and Breach, New York, 1986).

- <sup>5</sup>G. D. Watkins and R. P. Messmer, *Phys. Rev. Lett.* **25**, 656 (1970). Many defects have been modeled by means of cluster calculations. These are carried out with *ab initio* methods, empirical tight-binding methods, or with any of a number of different approximate schemes.
- <sup>6</sup>S. G. Louie, M. Schlüter, J. R. Chelikowsky, and M. L. Cohen, *Phys. Rev. B* **13**, 1654 (1976).
- <sup>7</sup>J. Bernholc, N. O. Lipari, and S. T. Pantelides, *Phys. Rev. Lett.* **41**, 895 (1978); *Phys. Rev. B* **21**, 3545 (1980).
- <sup>8</sup>G. A. Baraff and M. Schlüter, *Phys. Rev. Lett.* **41**, 892 (1978); *Phys. Rev. B* **19**, 4965 (1979).
- <sup>9</sup>R. Zeller and P. H. Dederichs, *Phys. Rev. Lett.* **42**, 1713 (1979).
- <sup>10</sup>A. R. Williams, P. J. Feibelman, and N. D. Lang, *Phys. Rev. B* **26**, 5433 (1982).
- <sup>11</sup>Y. Bar-Yam and J. D. Joannopoulos, *Phys. Rev. Lett.* **52**, 1129 (1984).
- <sup>12</sup>R. Car, P. J. Kelly, A. Oshiyama, and S. T. Pantelides, *Phys. Rev. Lett.* **52**, 1814 (1984).
- <sup>13</sup>G. A. Baraff and M. Schlüter, *Phys. Rev. B* **30**, 3460 (1984).
- <sup>14</sup>See, for example, the contributions in (a) *Defects in Semiconductors*, Proceedings of the 14th International Conference on Defects in Semiconductors, Paris, 1986, edited by H. J. von Bardeleben, *Materials Science Forum* **10–12** (Trans Tech, Aedermannsdorf, 1986); (b) *Defects in Semiconductors*, Proceedings of the 15th International Conference on Defects in Semiconductors, Budapest, 1988, edited by G. Ferenczi, *Materials Science Forum* **38–41** (Trans Tech, Aedermannsdorf, 1989).
- <sup>15</sup>U. von Barth and L. Hedin, *J. Phys. C* **5**, 1629 (1972).
- <sup>16</sup>D. R. Hamann, M. Schlüter, and C. Chiang, *Phys. Rev. Lett.* **43**, 1494 (1979).
- <sup>17</sup>G. B. Bachelet, D. R. Hamann, and M. Schlüter, *Phys. Rev. B* **26**, 4199 (1982).
- <sup>18</sup>R. C. Chaney, T. K. Tung, C. C. Lin, and E. E. Lafon, *J. Chem. Phys.* **52**, 361 (1970); E. E. Lafon, R. C. Chaney, and C. C. Lin, in *Computational Methods in Band Theory*, edited by P. M. Marcus, J. F. Janak, and A. R. Williams (Plenum, New York, 1972), p. 284.
- <sup>19</sup>J. Langlinsais and J. Callaway, *Phys. Rev. B* **5**, 124 (1972).
- <sup>20</sup>E. O. Kane, *Phys. Rev. B* **13**, 3478 (1976).
- <sup>21</sup>B. Holland, H. S. Greenside, and M. Schlüter, *Phys. Status Solidi B* **126**, 511 (1984).
- <sup>22</sup>J. R. Chelikowsky and S. G. Louie, *Phys. Rev. B* **29**, 3470 (1984).
- <sup>23</sup>G. F. Koster and J. C. Slater, *Phys. Rev.* **95**, 1165 (1954).
- <sup>24</sup>J. Callaway, *J. Math. Phys.* **5**, 783 (1964); *Phys. Rev.* **154**, 515 (1967).
- <sup>25</sup>C. Koenig, *J. Phys. F* **3**, 1497 (1973); R. Zeller, J. Deutz, and P. H. Dederichs, *Solid State Commun.* **44**, 993 (1982).
- <sup>26</sup> $\Delta N(z)$  is generally defined in (21) for complex energy  $z$ . By allowing the imaginary part of  $z$  to go to zero we obtain the change in the density of states  $\Delta N(\epsilon)$  for  $\epsilon$  within the band continua as well as the eventual bound-state energies when  $\epsilon$  falls within the forbidden gaps.
- <sup>27</sup>O. Gunnarsson, O. Jepsen, and O. K. Andersen, *Phys. Rev. B* **27**, 7144 (1983).
- <sup>28</sup>G. A. Baraff and M. Schlüter, *Phys. Rev. B* **28**, 2296 (1983); **30**, 1853 (1984).
- <sup>29</sup>P. J. Feibelman, *Phys. Rev. B* **35**, 2626 (1987).
- <sup>30</sup>In a metal, long-range oscillations in the screening charge (Friedel oscillations) arise due to the presence of a singularity in the static dielectric function for  $q = 2k_F$ , where  $k_F$  is the Fermi momentum. Although there is no such singularity in a semiconductor response function, there are long-range oscillations in the screening charge due to the nonuniformity of the medium (local-field effects).
- <sup>31</sup>U. von Barth and R. Car (unpublished).
- <sup>32</sup>A. Oshiyama, in *Proceedings of the Nineteenth International Conference on the Physics of Semiconductors*, edited by W. Zawadzki (Institute of Physics, Polish Academy of Sciences, Warsaw, 1988), p. 1059.
- <sup>33</sup>P. J. Feibelman, *Phys. Rev. B* **38**, 1849 (1988).
- <sup>34</sup>The effect on the total energy of adding to the screening charge of a defect of nominal charge  $-Q$ , an outer shell of charge  $Q/\epsilon_0$  having radius  $R$ , can be estimated from classical electrostatics to be  $Q^2/(2\epsilon_0^2 R)$ . For typical values of  $Q = 1$ ,  $\epsilon_0 = 10$ , and  $R = 10a_0$  this amounts to  $\sim 1$  mRy.
- <sup>35</sup>J. C. Slater and J. H. Wood, *Int. J. Quantum Chem. Suppl.* **4**, 3 (1971).
- <sup>36</sup>C. O. Ambladh and U. von Barth, *Phys. Rev. B* **13**, 3307 (1976).
- <sup>37</sup>J. Janak, *Phys. Rev. B* **18**, 7165 (1978).
- <sup>38</sup>J. C. Slater, *Quantum Theory of Molecules and Solids* (McGraw-Hill, New York, 1974), Vol. 4.
- <sup>39</sup>G. A. Baraff, E. O. Kane, and M. Schlüter, *Phys. Rev. Lett.* **43**, 956 (1979); *Phys. Rev. B* **21**, 5662 (1980).
- <sup>40</sup>G. A. Baraff, M. Schlüter, and G. Allan, *Phys. Rev. Lett.* **50**, 739 (1983).
- <sup>41</sup>U. Lindefelt, *Phys. Rev. B* **28**, 4510 (1983).
- <sup>42</sup>M. Scheffler, J. P. Vigneron, and G. B. Bachelet, *Phys. Rev. B* **31**, 6541 (1985).
- <sup>43</sup>P. J. Kelly, R. Car, and S. T. Pantelides, in *Defects in Semiconductors*, edited by H. J. von Bardeleben, *Materials Science Forum* **10–12** (Trans Tech, Aedermannsdorf, 1986), p. 115.
- <sup>44</sup>A. Antonelli and J. Bernholc, *Phys. Rev. B* **40**, 10643 (1989).
- <sup>45</sup>G. D. Watkins, in *Festkörperprobleme (Advances in Solid State Physics)*, edited by P. Grosse (Vieweg, Braunschweig, 1984), Vol. XXIV, p. 163.
- <sup>46</sup>P. N. Keating, *Phys. Rev.* **145**, 637 (1966).
- <sup>47</sup>G. D. Watkins and J. W. Corbett, *Phys. Rev.* **121**, 1001 (1961).
- <sup>48</sup>G. D. Watkins, J. W. Corbett, and R. S. McDonald, *J. Appl. Phys.* **53**, 7097 (1982).
- <sup>49</sup>P. J. Feibelman, *Phys. Rev. B* **33**, 719 (1986).
- <sup>50</sup>S. T. Pantelides and W. A. Harrison, *Phys. Rev. B* **13**, 2667 (1976).
- <sup>51</sup>P. J. Kelly, in *Proceedings of the Nineteenth International Conference on the Physics of Semiconductors*, edited by W. Zawadzki (Institute of Physics, Polish Academy of Sciences, Warsaw, 1988), p. 1027; *Defects in Semiconductors*, Proceedings of the 15th International Conference on Defects in Semiconductors, Budapest, 1988 (Ref. 14), p. 269.
- <sup>52</sup>R. Car, P. J. Kelly, A. Oshiyama, and S. T. Pantelides, *Phys. Rev. Lett.* **54**, 360 (1985).
- <sup>53</sup>G. A. Baraff and M. Schlüter, *Phys. Rev. Lett.* **55**, 1327 (1985).
- <sup>54</sup>R. Car, P. J. Kelly, A. Oshiyama, and S. T. Pantelides, *J. Electron. Mat.* **14a**, 269 (1985).
- <sup>55</sup>F. Beeler, M. Scheffler, O. Jepsen, and O. Gunnarsson, *Phys. Rev. Lett.* **54**, 2525 (1985).
- <sup>56</sup>C. M. Weinert and M. Scheffler, *Phys. Rev. Lett.* **58**, 1456 (1987).
- <sup>57</sup>F. Beeler and M. Scheffler, in *Defects in Semiconductors*, Proceedings of the 15th International Conference on Defects in Semiconductors, Budapest, 1988 (Ref. 14), p. 257.
- <sup>58</sup>Y. Bar-Yam and J. D. Joannopoulos, *Phys. Rev. B* **30**, 1844 (1984); **30**, 2216 (1984); *J. Electron. Mat.* **14a**, 261 (1985).
- <sup>59</sup>K. C. Pandey, *Phys. Rev. Lett.* **57**, 2287 (1986).
- <sup>60</sup>J. Dabrowski and M. Scheffler, *Phys. Rev. Lett.* **60**, 2183

- (1988); D. J. Chadi and K. J. Chang, *ibid.* **60**, 2187 (1988).
- <sup>61</sup>F. Buda, G. L. Chiarotti, R. Car, and M. Parrinello, *Phys. Rev. Lett.* **63**, 294 (1989).
- <sup>62</sup>C. G. van de Walle, Y. Bar-Yam, and S. T. Pantelides, *Phys. Rev. Lett.* **60**, 2761 (1988); P. J. H. Denteneer, C. G. van de Walle, and S. T. Pantelides, *ibid.* **62**, 1884 (1989).
- <sup>63</sup>J. Bernholc, A. Antonelli, T. M. Del Sole, Y. Bar-Yam, and S. T. Pantelides, *Phys. Rev. Lett.* **62**, 1884 (1989).
- <sup>64</sup>J. Ihm, A. Zunger, and M. L. Cohen, *J. Phys. C* **12**, 4409 (1979).
- <sup>65</sup>M. T. Yin and M. L. Cohen, *Phys. Rev. B* **26**, 5668 (1982).
- <sup>66</sup>C. G. van de Walle, P. J. H. Denteneer, Y. Bar-Yam, and S. T. Pantelides, *Phys. Rev. B* **39**, 10791 (1989); P. J. H. Denteneer, C. G. van de Walle, and S. T. Pantelides, *ibid.* **39**, 10809 (1989).
- <sup>67</sup>W. Frank, U. Gösele, H. Mehrer, and A. Seeger, in *Diffusion in Solids: Recent Developments*, edited by G. E. Murch and A. S. Nowick (Academic, New York, 1984).
- <sup>68</sup>G. D. Watkins, in *Deep Centers in Semiconductors* (Ref. 4).
- <sup>69</sup>S. Dannefaer, P. Mascher, and D. Kerr, *Phys. Rev. Lett.* **56**, 2195 (1986).
- <sup>70</sup>J. Bernholc, A. Antonelli, C. Wang, R. F. Davis, and S. T. Pantelides, in *Defects in Semiconductors*, Proceedings of the 15th International Conference on Defects in Semiconductors, Budapest, 1988 (Ref. 14), p. 713.
- <sup>71</sup>C. S. Nichols, C. G. van de Walle, and S. T. Pantelides, *Phys. Rev. B* **40**, 5484 (1989).
- <sup>72</sup>C. S. Nichols, private communication.
- <sup>73</sup>M. Saito and A. Oshiyama, *Phys. Rev. B* **38**, 10711 (1988).
- <sup>74</sup>L. C. Snyder and J. W. Corbett, *J. Electron. Mat.* **14a**, 693 (1985).
- <sup>75</sup>L. C. Snyder, J. W. Corbett, P. Deák, and R. Wu, in *New Developments in Semiconductor Physics*, edited by G. Ferenczi and F. Beleznyay, Lecture Notes in Physics Vol. 301 (Springer, Berlin, 1988), p. 147.